AD-A081 474 PAYNE INC ANNAPOLIS MD F/G 13/10
A NOTE ON THE EFFICIENCY POTENTIAL OF SEMI-SUBMERGED SHIPS. REV--ETC(U)
JUL 76 P R PAYNE N00600-76-C-1761
UNCLASSIFIED WORKING PAPER-196-2-REV-1 NL

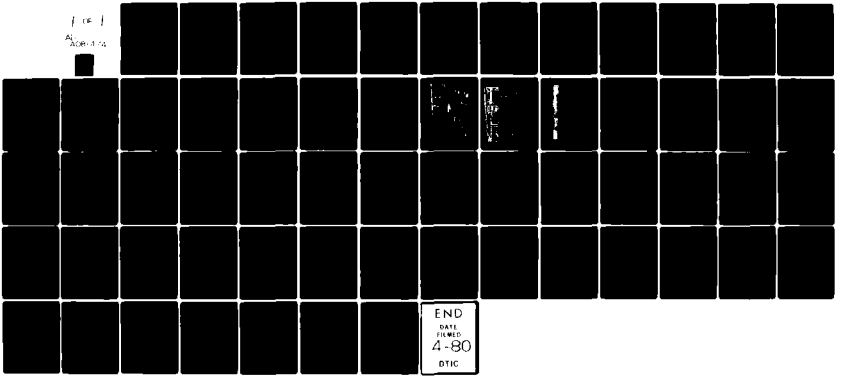

END
DATE FILMED
4-80
DTIC

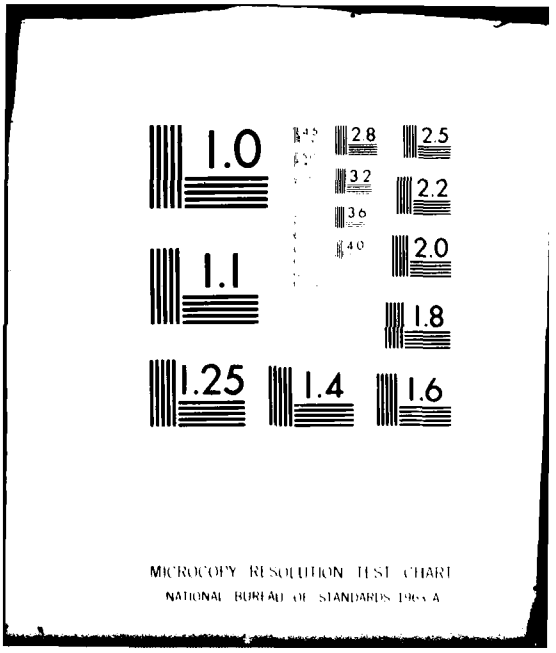
1.0
2.8
2.5
3.2
2.2
3.6
4.0
2.0
1.1
1.8
1.25
1.4
1.6
MICROCOPY RESOLUTION TEST CHART
NATIONAL BUREAU OF STANDARDS 1963 A

UNCLASSIFIED
SECURITY CLASSIFICATION OF THIS PAGE (When Data Entered)

REPORT DOCUMENTATION PAGE

READ INSTRUCTIONS BEFORE COMPLETING FORM

1. REPORT NUMBER: W.P. No. 196-2 Rev 1
2. GOVT ACCESSION NO.
3. RECIPIENT'S CATALOG NUMBER
4. TITLE (and Subtitle): A Note on the Efficiency Potential of Semi-Submerged Ships
5. TYPE OF REPORT & PERIOD COVERED
6. PERFORMING ORG. REPORT NUMBER
7. AUTHOR(s): Peter R. Payne
8. CONTRACT OR GRANT NUMBER(s): ~~N00600~~-76-C-1761 N00600
9. PERFORMING ORGANIZATION NAME AND ADDRESS: Payne, Inc. Annapolis, Maryland 21401
10. PROGRAM ELEMENT, PROJECT, TASK AREA & WORK UNIT NUMBERS
11. CONTROLLING OFFICE NAME AND ADDRESS
12. REPORT DATE: July 1976
13. NUMBER OF PAGES: 55
14. MONITORING AGENCY NAME & ADDRESS (if different from Controlling Office)
15. SECURITY CLASS. (of this report): Unclassified
15a. DECLASSIFICATION/DOWNGRADING SCHEDULE

16. DISTRIBUTION STATEMENT (of this Report)

Unlimited and approved for Public release.

17. DISTRIBUTION STATEMENT (of the abstract entered in Block 20, if different from Report)

18. SUPPLEMENTARY NOTES

This report used by OP96V in their study: Advanced Naval Vehicle Concepts Evaluation.

19. KEY WORDS (Continue on reverse side if necessary and identify by block number)

Advanced Naval Vehicle Concepts Evaluation
ANVCE
Technology Assessment
Semi-Submerged Ship
Lift/Drag Ratio
SWATH

20. ABSTRACT (Continue on reverse side if necessary and identify by block number)

This paper is concerned mainly with the "lift/drag" ratio (L/D) which could be achieved with semi-submerged ships ($S^3_{(1)}$). Given that the motion in a seaway can be very small, then L/D is far the most important factor in any comparison with other forms of vehicle. That motions can be less than for conventional ships has been clearly shown by a number of eminent workers over the last thirty years. We suggest here, in fact, that motions could be essentially zero, if one is prepared to accept a form which has negligible

DD FORM 1 JAN 73 1473 EDITION OF 1 NOV 65 IS OBSOLETE

UNCLASSIFIED
SECURITY CLASSIFICATION OF THIS PAGE (When Data Entered)

20. (cont.)

hydrostatic pitch and roll stiffness when underway, relying on dynamic pressure forces on stabilizer foils for stability. We conclude that in medium and large sizes, S_{Δ}^{3} offers the possibility of very high L/D ratios in the intermediate speed range around 60 knots, and large S_{Δ}^{3} may be competitive at 100 knots. The poor showing to date seems to be principally due to designs which have the submerged hull too close to the surface, struts which are very thick and/or have large wetted area, and insufficient development work on reducing interference drag.

2059

Payne inc.

1910 Forest Drive • Annapolis, Md. 21401 • (301) 268-6150

Working Paper No. 196-2
July 1976
Revision 1

A NOTE ON THE EFFICIENCY POTENTIAL OF SEMI-SUBMERGED SHIPS

by

Peter R. Payne

Payne Inc.

1910 Forest Drive • Annapolis, Md. 21401

TABLE OF CONTENTS

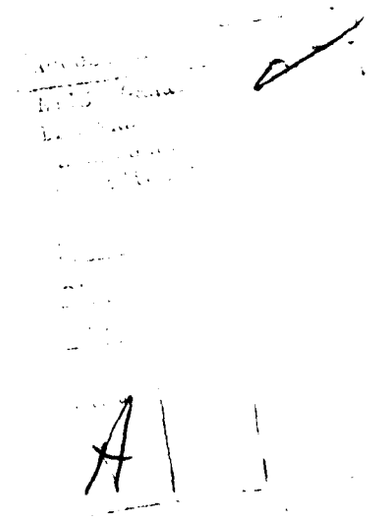

SUMMARY AND CONCLUSIONS

This paper is concerned mainly with the "lift/drag" ratio (L/D) which could be achieved with semi-submerged ships (S^3). Given that the motion in a seaway can be very small, then L/D is by far the most important factor in any comparison with other forms of vehicle. That motions can be less than for conventional ships has been clearly shown by a number of eminent workers over the last thirty years. We suggest here, in fact, that motions could be essentially zero, if one is prepared to accept a form which has negligible hydrostatic pitch and roll stiffness when underway, relying on dynamic pressure forces on stabilizer foils for stability. The struts which support the above-water portion of the ship can then be sized by structural considerations only. Of course, this implies that the upper hull will descend to the water surface for low speed operation, as indicated in Figure 1. In many ways, operation of the Figure 1 configuration would be similar to operation of a hydrofoil, and there are some interesting and potentially rewarding trade-offs to be made between buoyant and dynamic lift. Note also that the ability to employ a multiplicity of struts means that the upper size limitations of a conventional hydrofoil are evaded.

The SWATH configuration in Figure 1 has $\sqrt{2}$ times more wetted area than the minimum wetted area possible, so we show an alternative configuration in Figure 2. This was first suggested by R.W. Priest in the fifties,* although with struts large enough to provide hydrostatic stability.

The hydrodynamic efficiency (L/D) of such a single body is shown in Figures 3 - 5, based on calculations described later in this paper. If we select 60 knots as the speed of interest, we see that L/D increases markedly with size, but also with depth of immersion in the larger sizes. For Δ = 2000 tons,

$$L/D \simeq 10 \text{ with the body top at the surface}$$

$$\simeq 20 \text{ with the body top 48 feet below the surface.}$$

For Δ = 20,000 tons, there's not much difference when the draft is shallow, but a total draft of 161 feet gives L/D = 39. L/D = 50 is theoretically attainable, if the body is deep enough. These figures are very attractive by comparison with other types of advanced vehicle.

So far, we have only considered conventional underwater bodies. Suppose now we halve the skin friction coefficient in some way; either by polymer injection** or by appropriately shaping the body. The ultra-low drag underwater bodies† are an example of such drag reduction by shaping, by virtue of extensive

---

*Reported by Boericke[1].

** See Van Mater[2] for example.

† Payne[3] describes the antecedants of this technology.

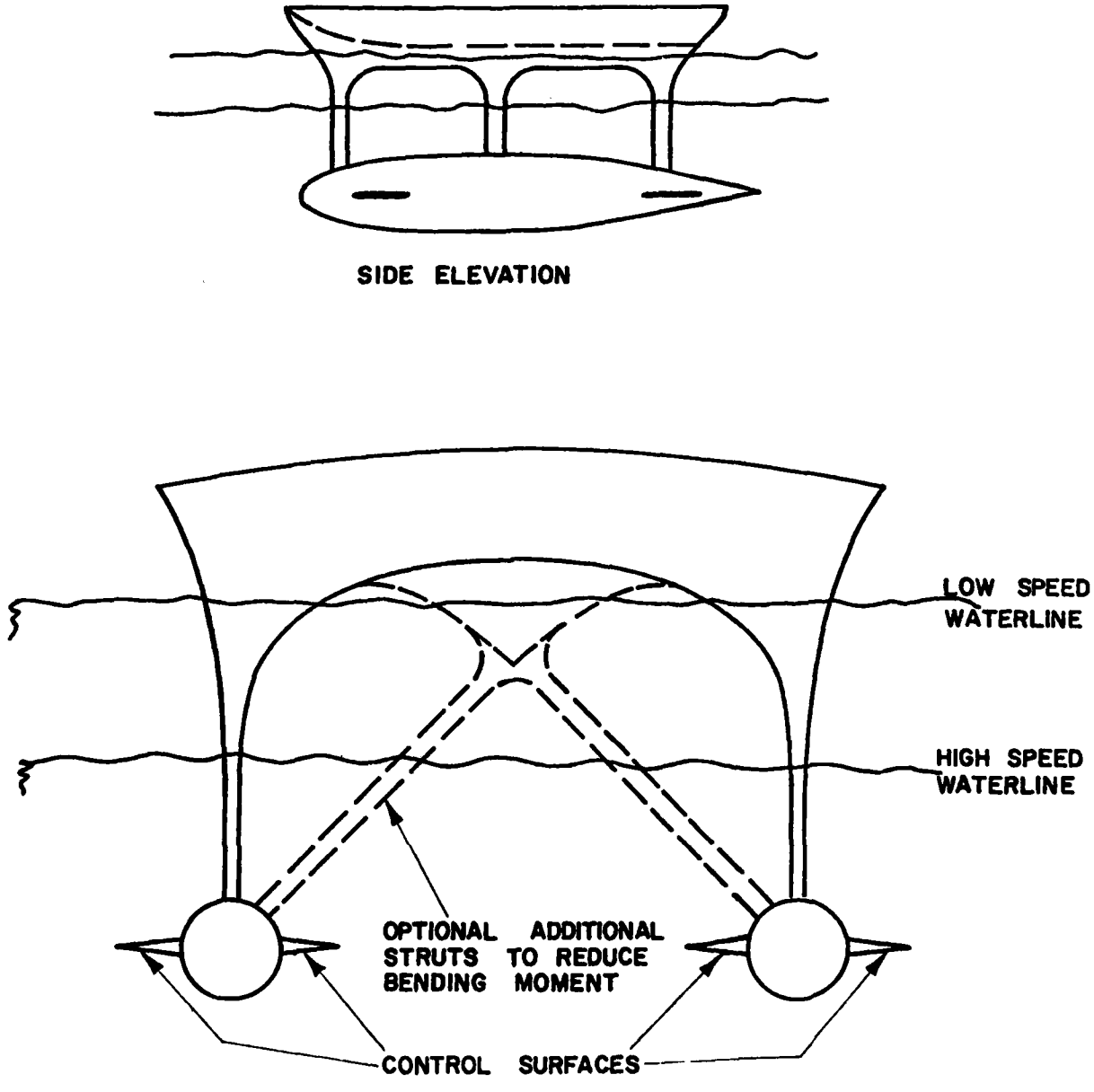

Figure 1. A Small Waterplane Twin Hull (SWATH) Configuration Which Becomes "Foil-Borne" for High Speed Operation.

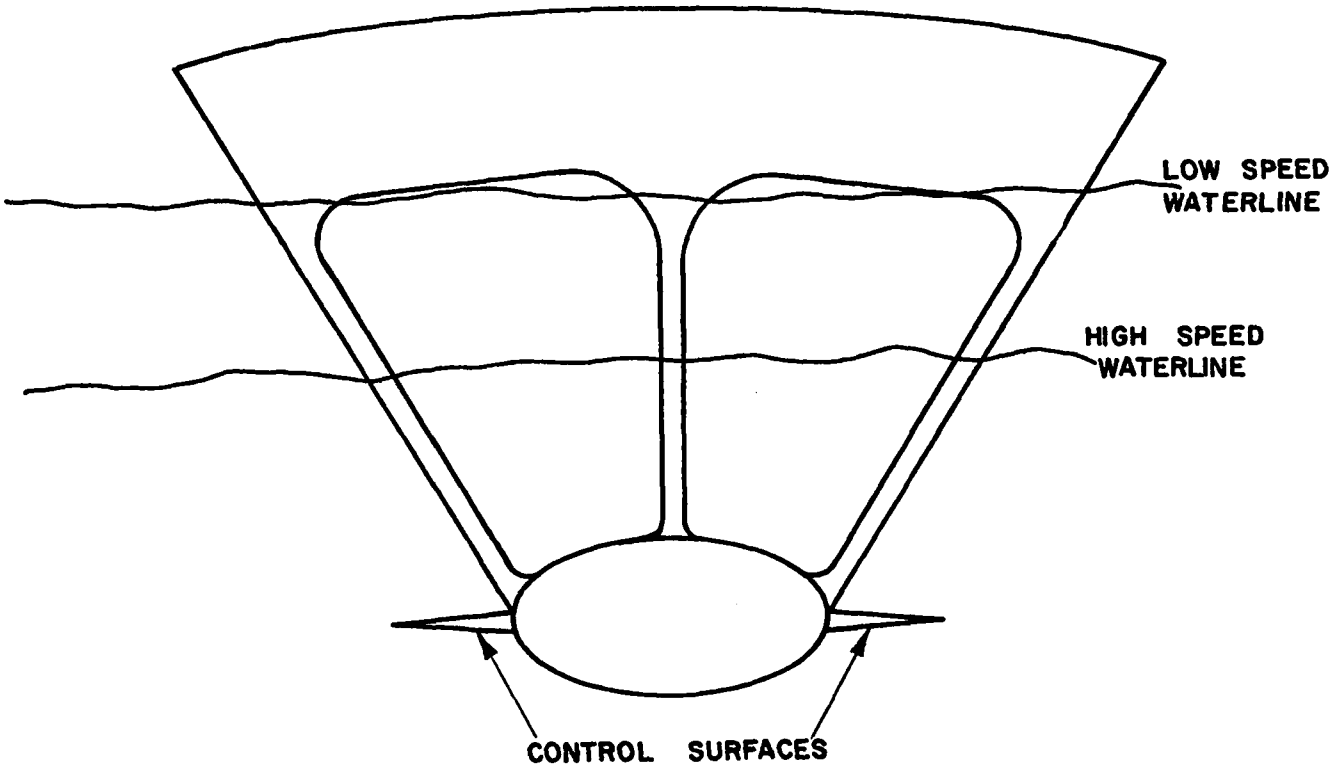

Figure 2. A Single Submerged Body.

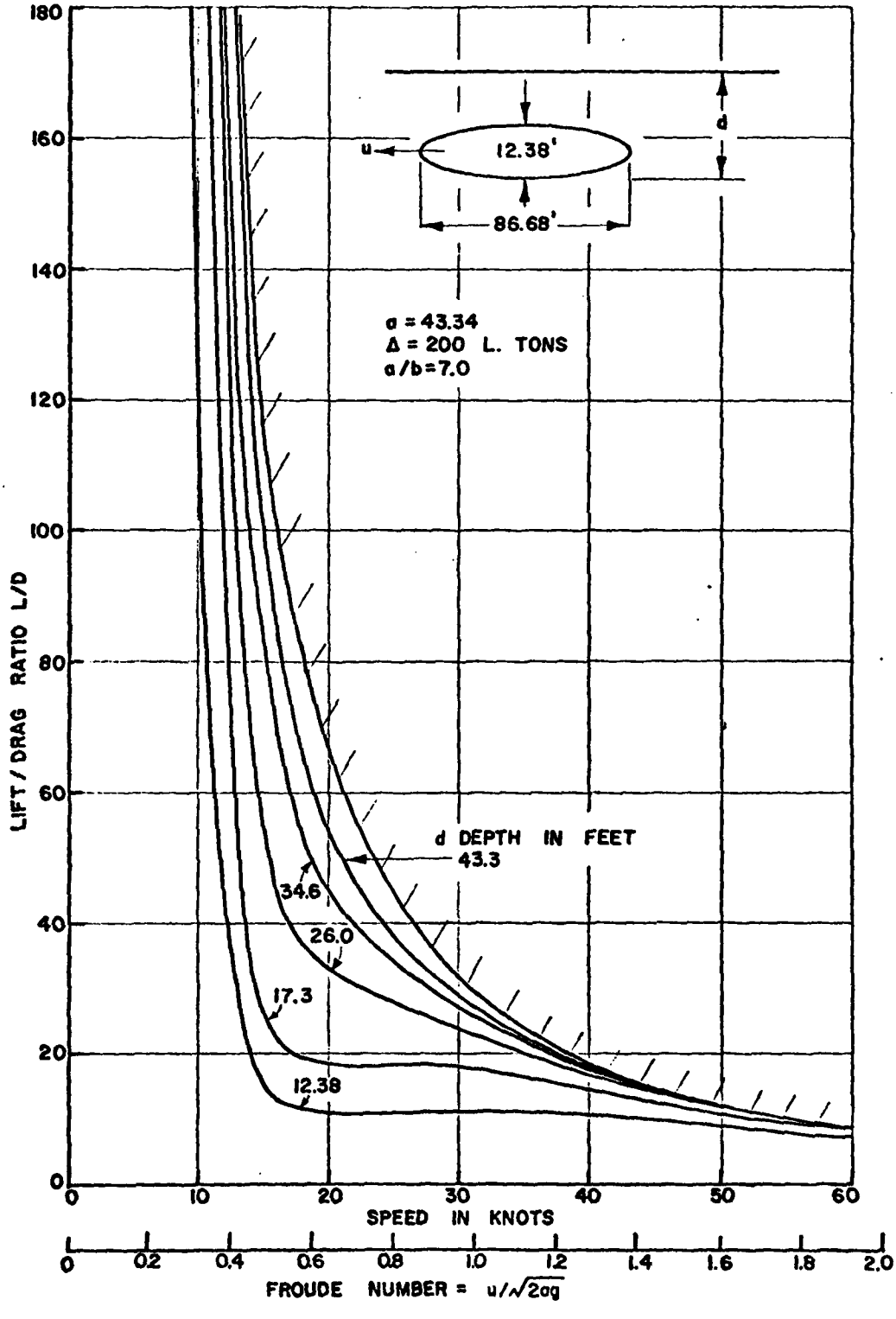

Figure 3. Performance of a 200 Ton Submerged Body.

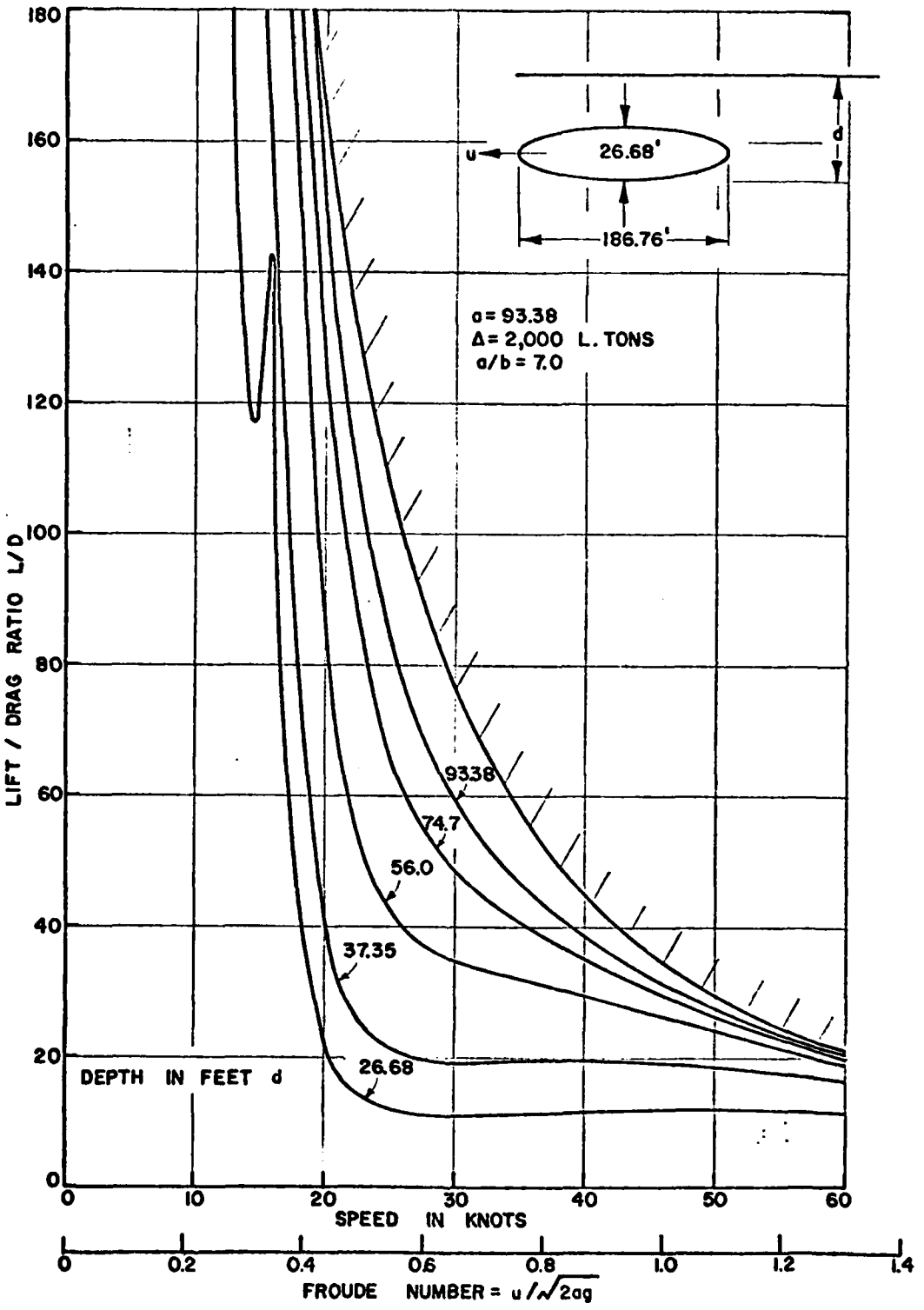

Figure 4. Performance of a 2000 Ton Submerged Body.

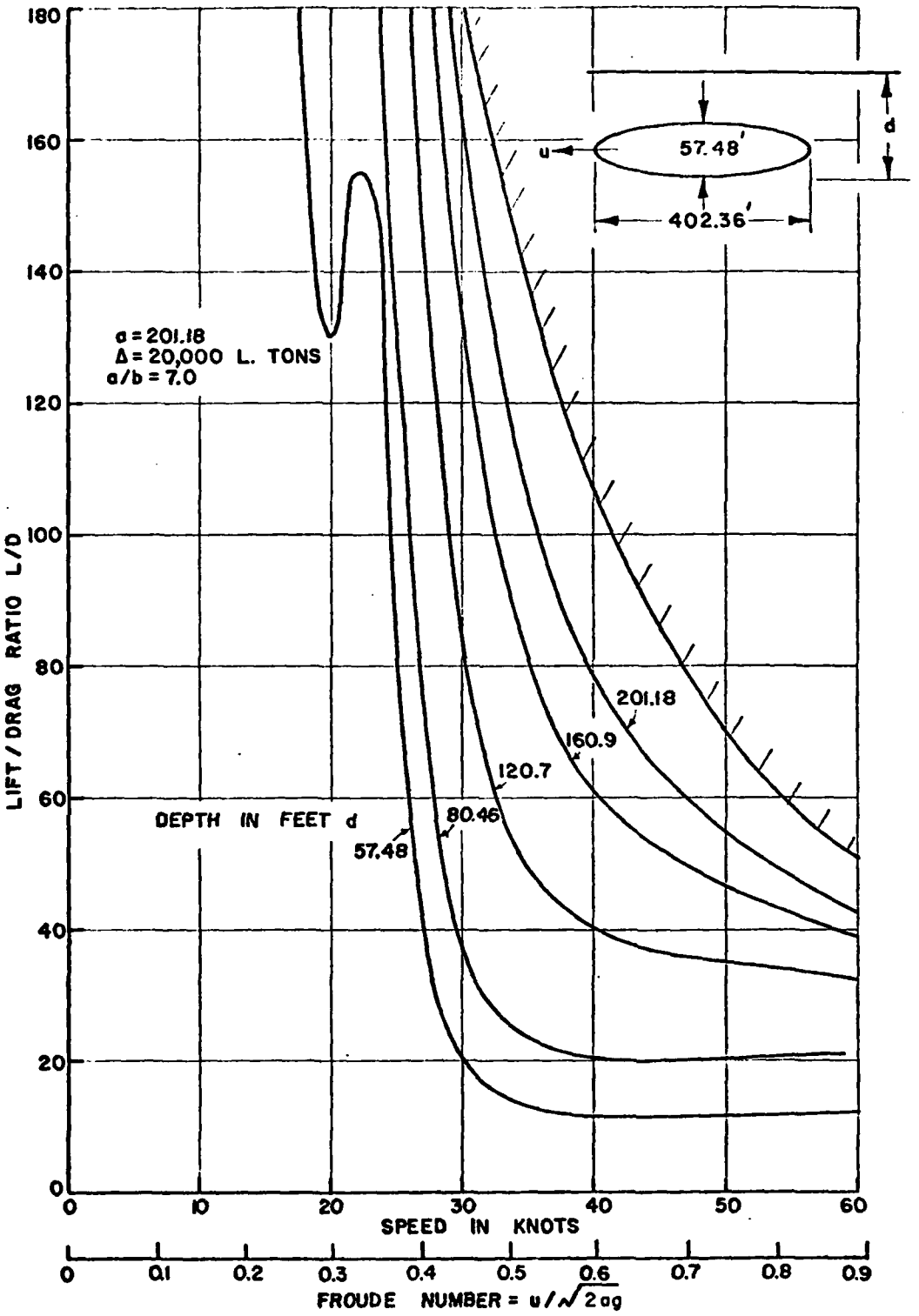

Figure 5. Performance of a 20,000 Ton Submerged Body.

laminar flow in their boundary layers. Perhaps a more practical possibility for S^3 is to design for a "tired," low friction turbulent boundary layer over most of the body. Stratford[4] has demonstrated such a flow experimentally, and while no one has yet investigated the technology exhaustively for external flows, it would appear to offer some promise.

A third alternative is drag reduction by injected air lubrication.

If such a halving of the skin friction coefficient is achieved, then the L/D ratios for the three different displacements become as shown in Figures 6 - 8. Even the 200 ton size is now competitive with other vehicles at 60 knots (L/D ≈ 17) while values as high as L/D = 80 are feasible in the 20,000 ton size.

It should be emphasized that all of these values will be degraded by

- Strut drag.
- Foil drag.
- Resistance of any other appendages.

By careful design, however, we can minimize the penalties involved. But since strut size dominates strut drag, and strut size depends principally on structural loads, we have not attempted to include estimates for these parasitic items in this paper.

We conclude that in medium and large sizes, S^3 offers the possibility of very high L/D ratios in the intermediate speed range around 60 knots, and large S^3 may be competitive at 100 knots. The poor showing to date seems to be principally due to designs which have the submerged hull too close to the surface, struts which are very thick and/or have large wetted area, and insufficient development work on reducing interference drag.

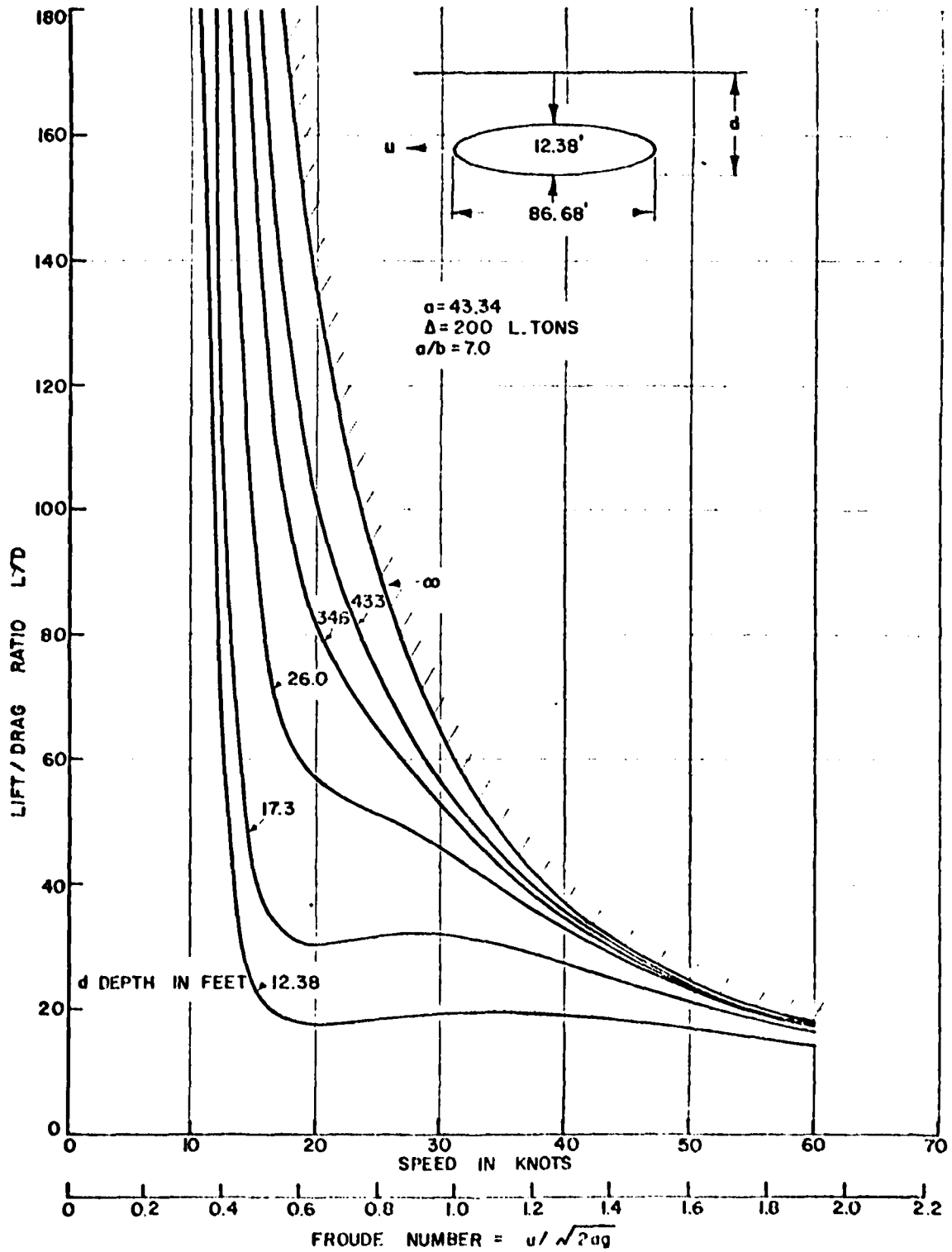

Figure 6. Performance of a 200 Ton Submerged Body if the Skin Friction Coefficient is Halved.

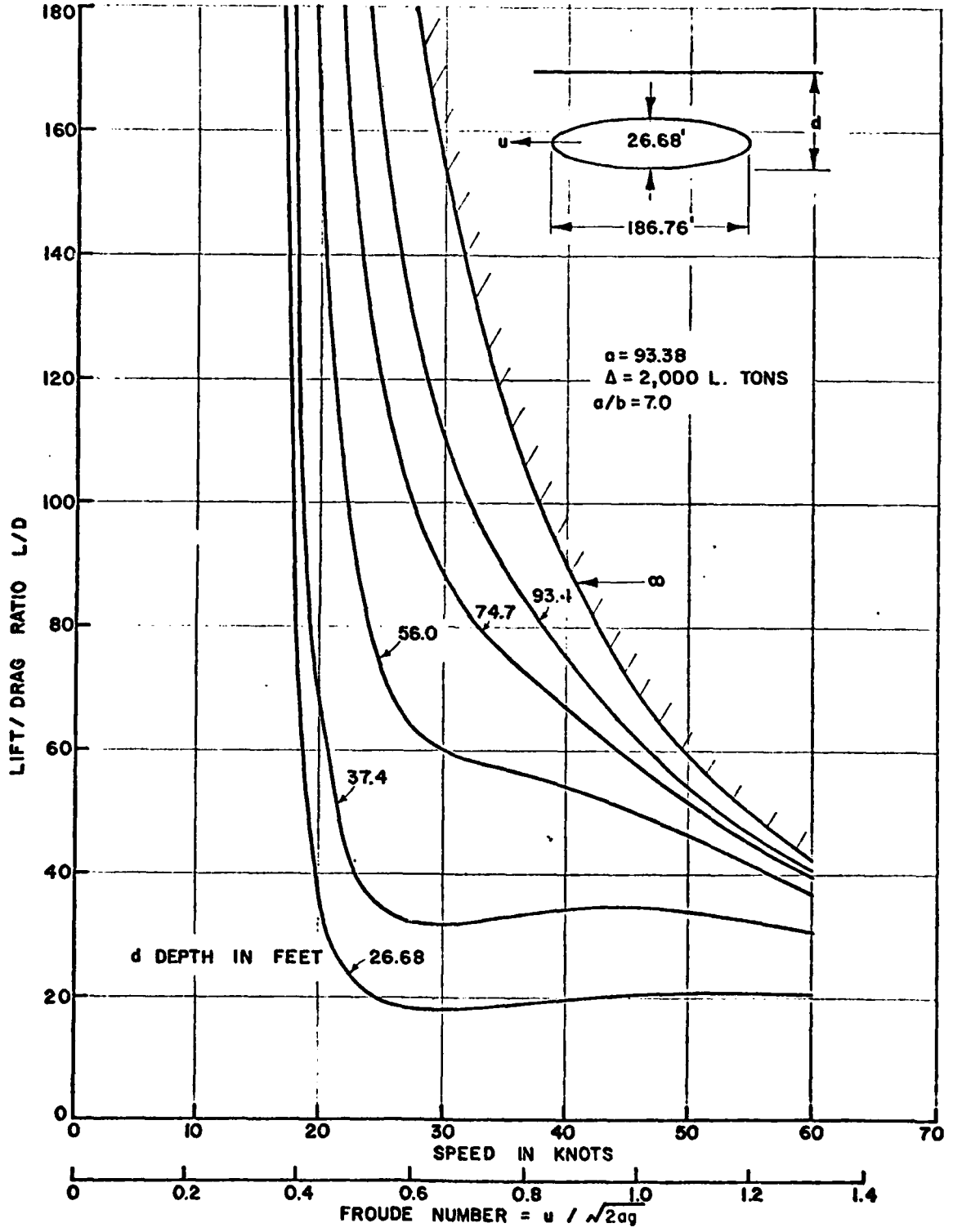

Figure 7. Performance of a 2000 Ton Submerged Body if the Skin Friction Coefficient is Halved.

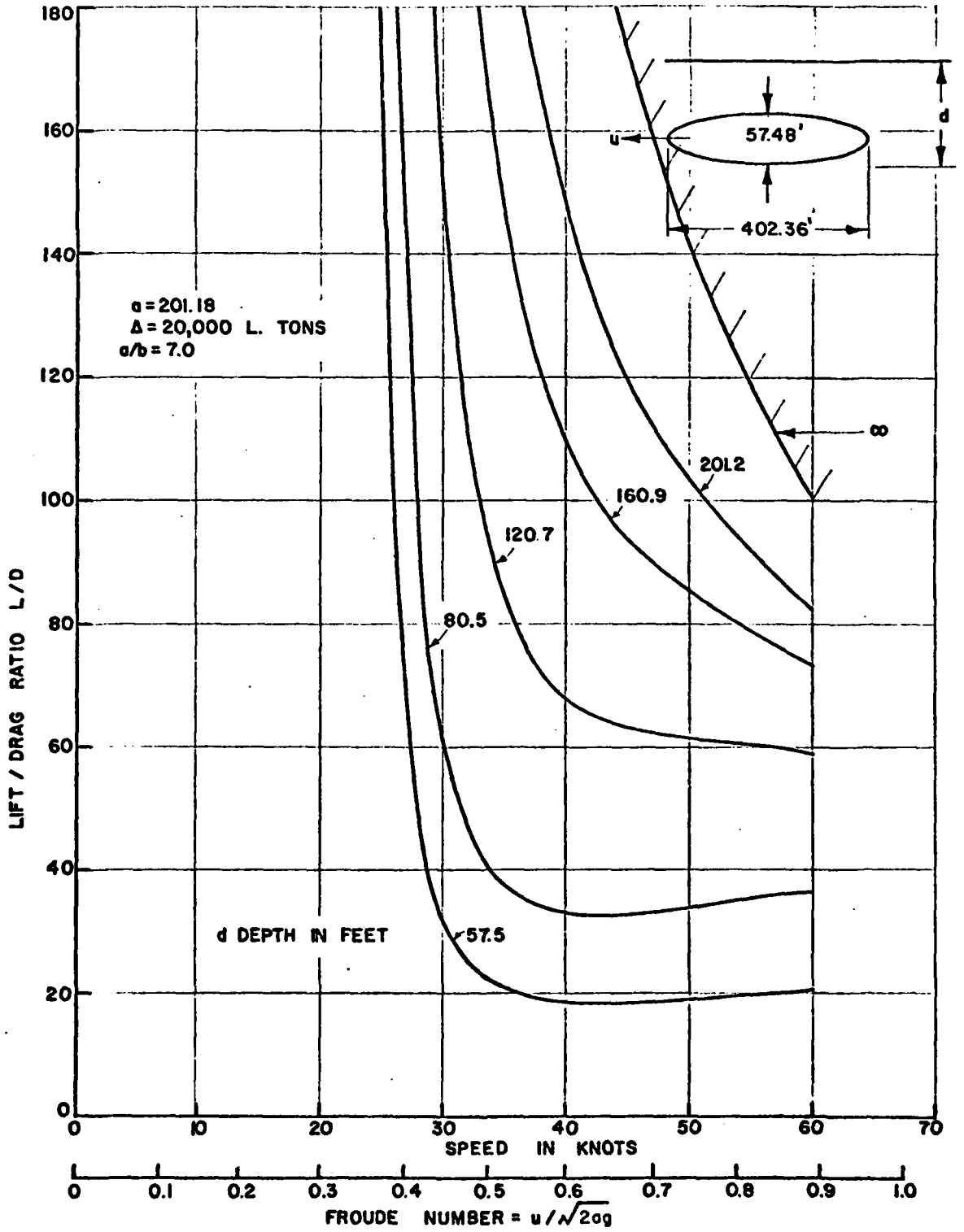

Figure 8. Performance of a 20,000 Ton Submerged Body if the Skin Friction Coefficient is Halved.

A VERY BRIEF HISTORY OF SEMI-SUBMERGED SHIPS

There does not seem to be any totally satisfactory name for what we are discussing. The abbreviation S^3 does at least have the merit of extreme brevity, and so we employ it here. But we are really talking about a ship which has low self-making wave drag, and a reduced response to the seaway. A "small waterplane area" ship will generally have both these virtues, but the description is very imprecise. Also there is at least one other way of achieving the same result, as we shall see.

The first patent for S^3 was awarded to Reuben N. Perley (1922) for a submerged monohull with surface-piercing struts forward and aft. A similar ship with a single strut (the "Shark form") was patented by Rudolf Engleman in 1937. A modern SWATH configuration was patented (in England) by Frederick G. Creed in 1944. Thus there is nothing particularly "new" about the basic idea or concept. The problem has been in assessing its virtues and vices.

It would seem that the earliest studies in this country were carried out by a group in BuShips (Code 420) under Owen Oakley, in the early fifties. Boericke[1] summarizes much of the work done by this unusually creative team, which included Robert W. Priest, David Winter, James L. Mills and others. Unfortunately, they were apparently unable to arouse any interest in supporting the broad-based R&D effort which would have been required to select the best among their various proposed configurations and then to develop it. Figure 9 depicts some of the configurations studied at this time.

From a different vantage point, Lewis' studies[5] of seakeeping in the mid-fifties led to the first semi-submerged ship (S^3) described as such, and a form which he patented in 1959.[6] The lines are given in Figure 10. This was the first time, apparently, that a form had been consciously designed for supercritical operation in head seas; although supercritical operation was known to be possible with conventional forms under certain rather special conditions. Insofar as one can tie it down to one individual, Lewis was clearly the inventor of the supercritical ship.

The work of this intellectually fruitful decade was summarized in a number of important papers which appeared in the period 1959-1962. Mandel's[7] study, and that of Lewis and Breslin[8] are the best and the most complete. But Mandel's statement that "none of the new ship types . . . is likely to supplant more traditional ships and aircraft . . ." may have discouraged some further work, because it was so easily taken out of context.

At this point, one might say that the most severe seakeeping problem - high speed in head seas - had been solved by Lewis' invention of the supercritical ship (SCS) and that this concept could be applied to some of the configurations already proposed. But the monohull SCS was very tender in roll, had insufficient deck space for many purposes, and experienced rather extreme motions at resonance.

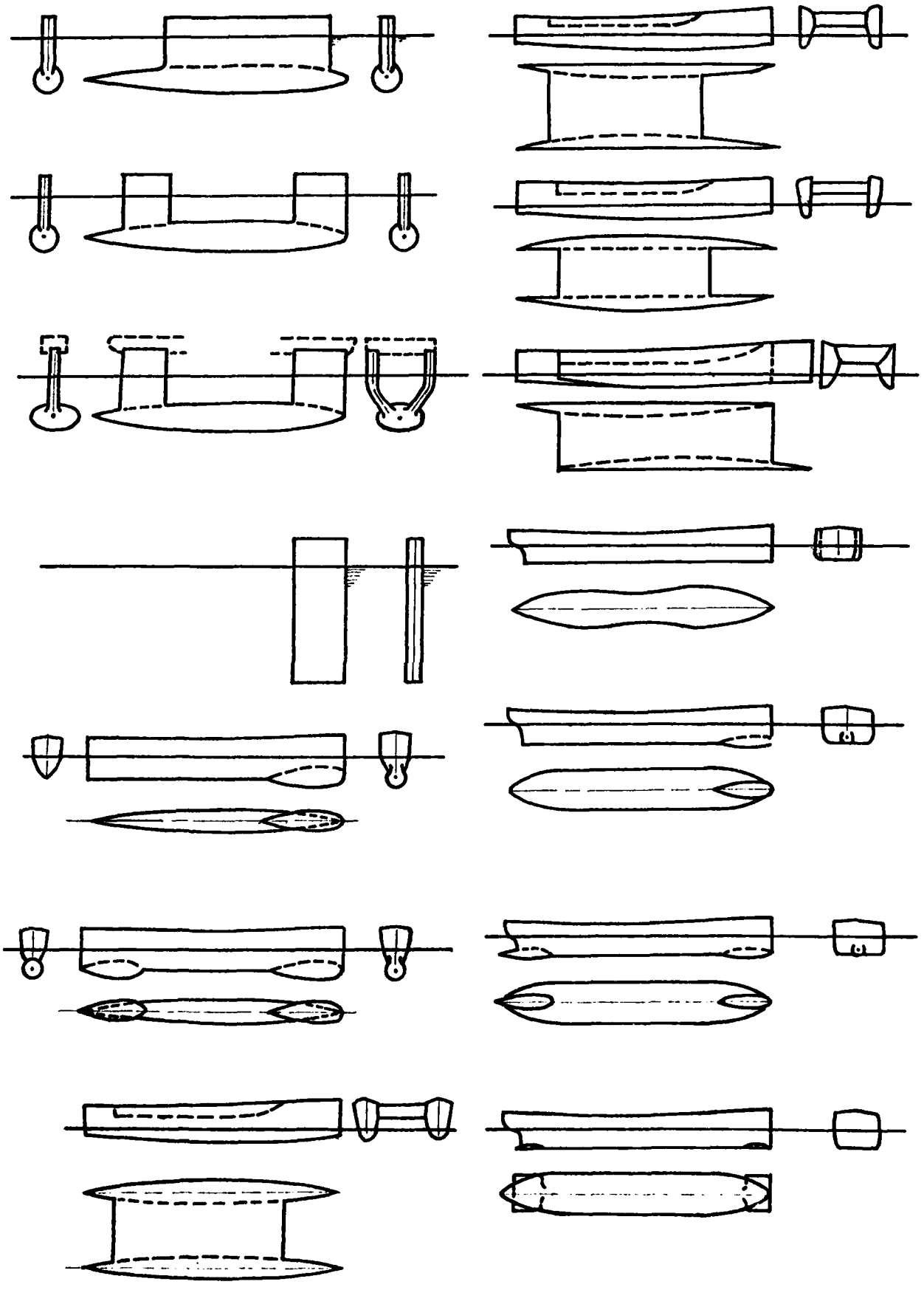

Figure 9. Configurations Studied by the Code 420 (Preliminary Design) Team in the Early Fifties. (From Bocricke[1])

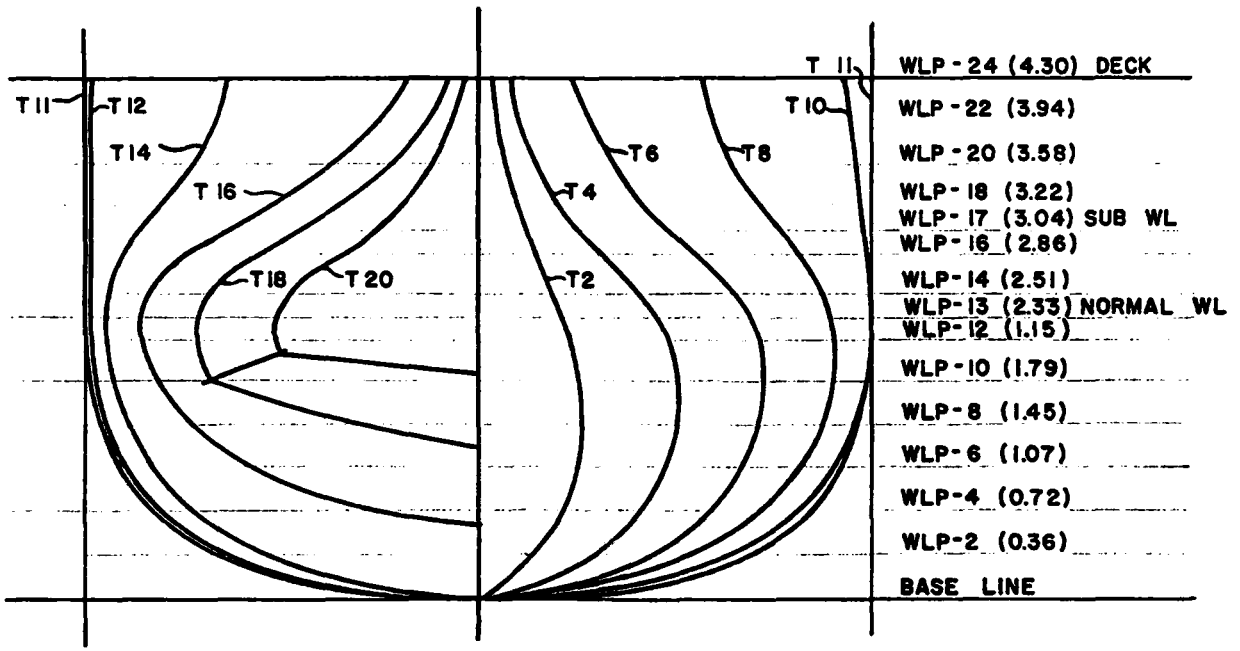

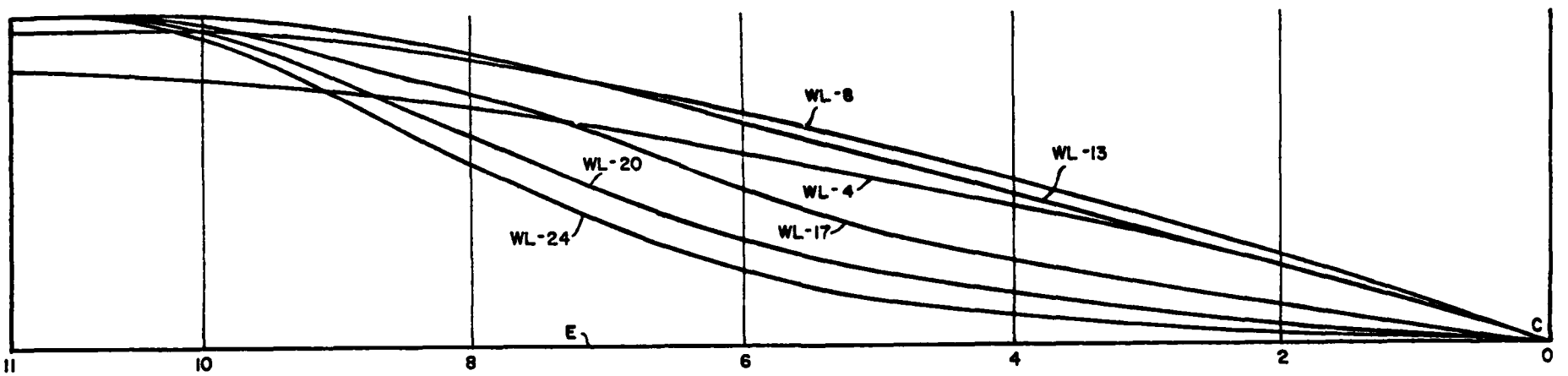

Figure 10. Lines of Lewis' Semi-Submerged Ship.

In the period 1964-66, Payne built two small, manned, supercritical catamarans (FICAT I and II) which avoided the first two of these three problems. The first of these craft is shown in Figure 11. A reduction in wave drag was achieved partly by the reduction in individual hull beam which is permitted by the catamaran configuration, and partly by cancellation interference of the wave trains from each hull. In other words, interference was substituted for submergence of the main buoyancy volume. This avoided some of the practical problems associated with S^3 struts, excessive draft, etc., and resulted in a more conventional ship.

The two FICAT's were operated "at sea" in the Chesapeake area for some hundreds of hours, during the years 1965-66, under widely varying conditions. Model tests (Figure 12) were also conducted, and it seemed clear that at least a 50% wave drag cancellation was being achieved for all Froude numbers above about 0.5, with some evidence of total cancellation at $F = 0.7$.[9] The FICAT's were the first SCS configurations to be analyzed theoretically[10,11,12] so far as resistance was concerned. Band found generally good agreement between Michell's wave drag integral and experiment, including wave drag calculated from photographs of the local surface elevation.

Despite the significant progress made, the Payne team was never able to find support for its research, which was therefore discontinued in early 1969, so that attention could be concentrated on supercritical planing hulls. A definitive assessment of FICAT vis-a-vis other configurations was never made, and so this must remain a question mark.

Coincident with Payne's departure from the field, Leopold[13,14] re-introduced the Creed configuration and built the first Litton TRISEC[15] man-carrying model. This was the first true S^3 actually reduced to practice, and its seakeeping ability was very impressive. The problem of excessive motions near resonance was solved by using inclined active foils which acted as both rudders and pitch angle control.

Litton was also unsuccessful in obtaining funding to pursue the research, but the basic concept has since been an ongoing project in the Navy, principally at NSRDC and NAVSEC.

Shortly after Leopold, Lang[16,17] patented some very innovative improvements, and was later able to build a 190 ton "manned model." Again, because of lack of funds, this design was not "optimized," and has a much higher resistance than the minimum possible. Lang adopted and improved the active foil stabilization concept, and linked it to a simple autopilot to achieve minimum motions at all speeds.

In this present paper, we have suggested that, since active stabilization is essential while underway, one might as well dispense with hydrostatic stability and thus avoid the rather severe resistance penalties which it imposes. We also suggest that the hulls should be much deeper in the water if high efficiency is to be achieved. Then, as a final improvement, the operational limitations imposed by this deep draft can be ameliorated by hinging the strut assembly in such a way that the above and underwater hulls can be brought together for low speed, low draft operation. Although there may be some size limitations to this last suggestion, the basic technology is not far removed from that used in the new variable wing sweep bombers.

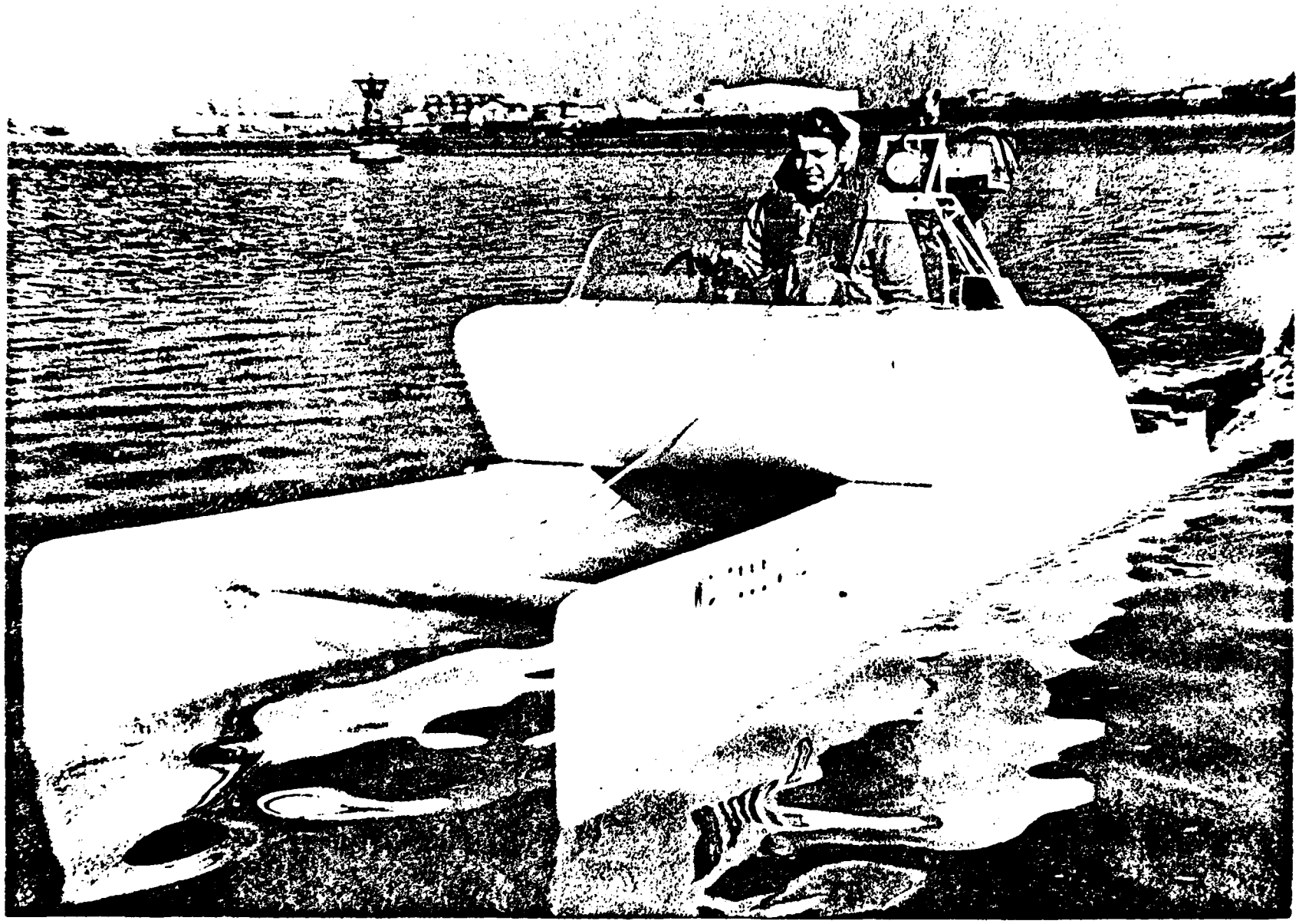

Figure 11. FICAT I Model with Air Propulsion.

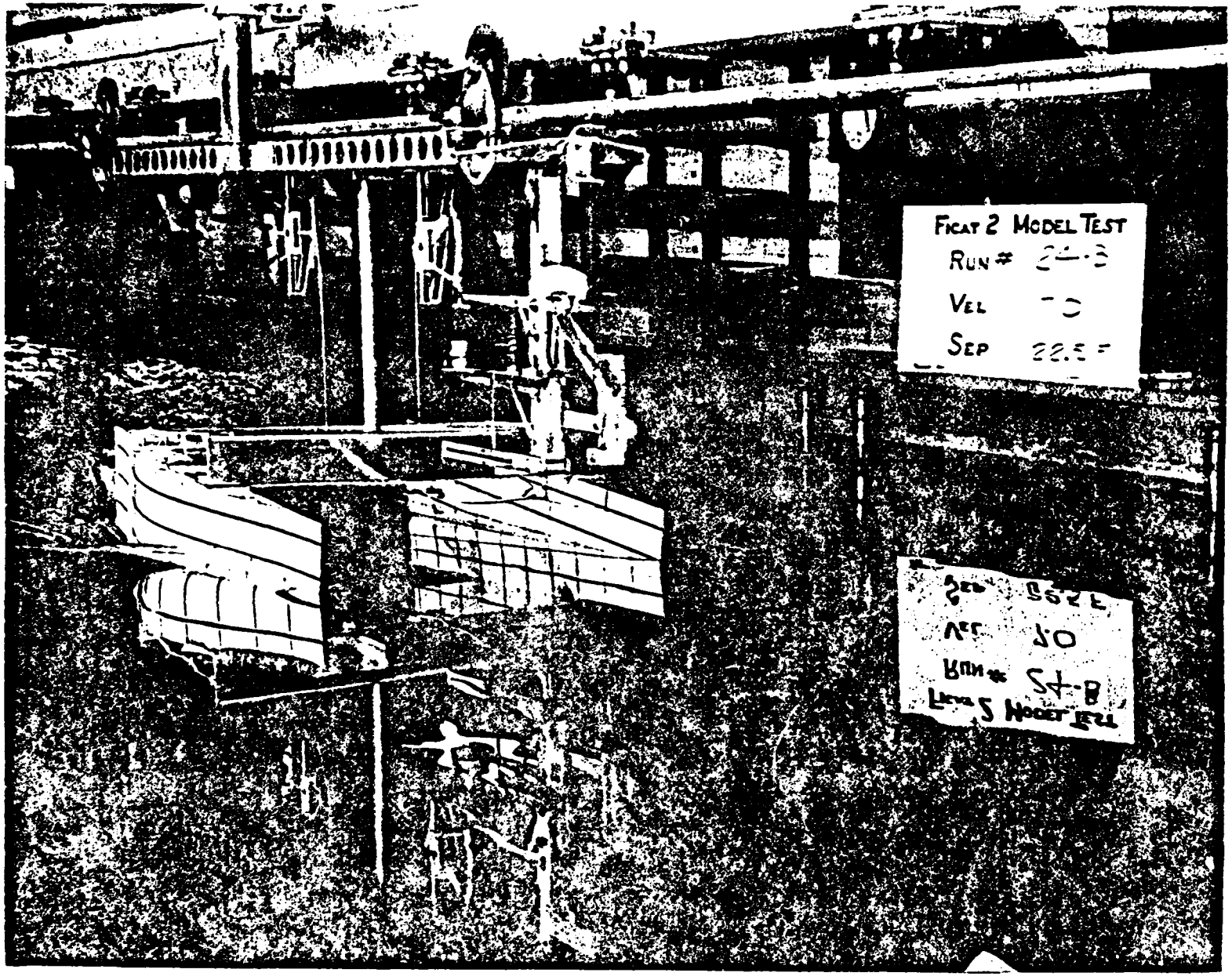

Figure 12. A Model FICAT Experiencing Bow "Dig In" During Tank Testing. The Floats Have Been Reversed for This Experiment.

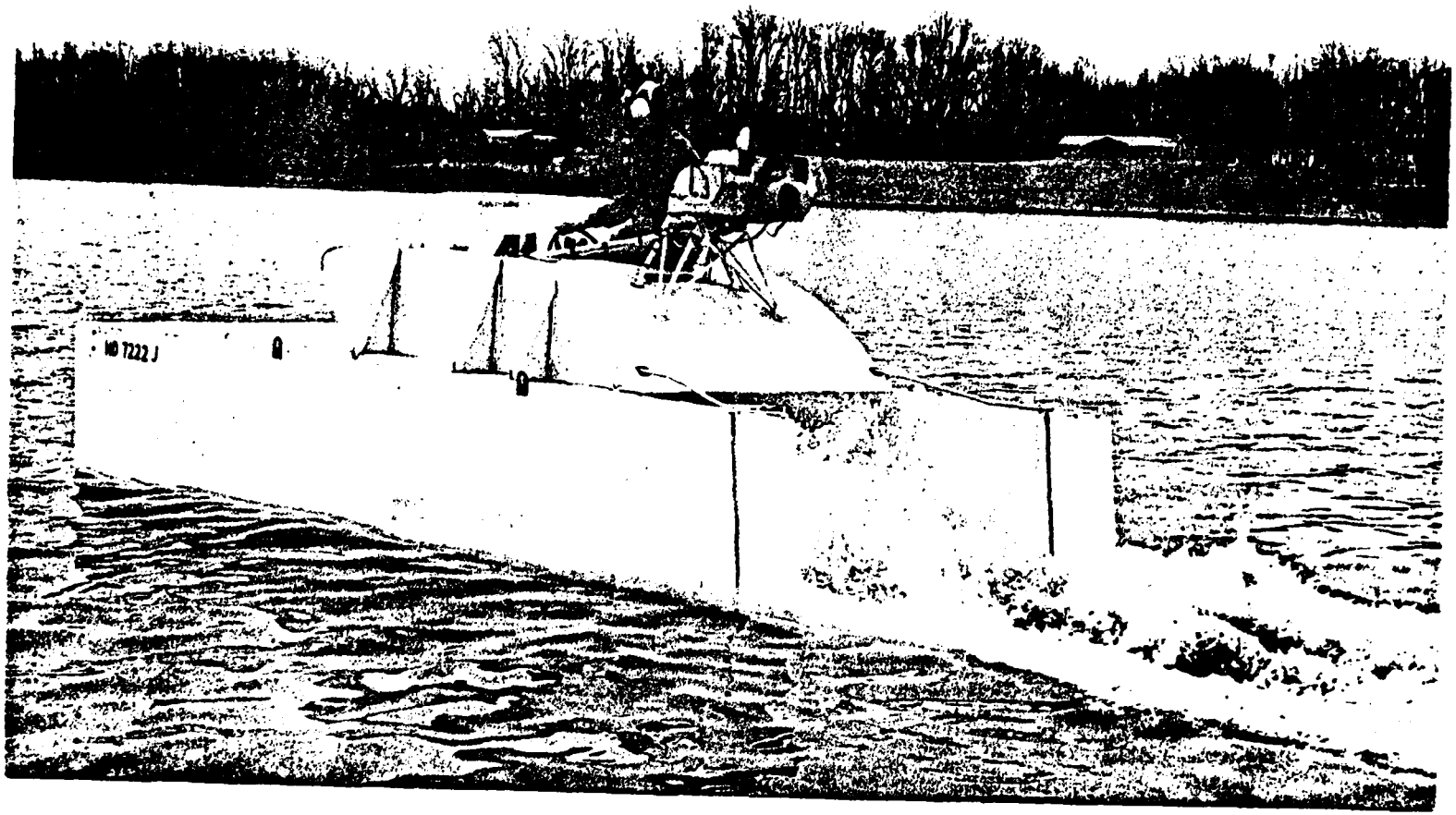

Figure 13. FICAT II at Speed. As the first manned supercritical ships, the FICAT's demonstrated the practicality of the concept under "real world" conditions in the Chesapeake Bay.

THE PERFORMANCE CALCULATIONS

Oddly enough, the basic theoretical tools for an overview assessment were developed by Havelock prior to the need for them. The four relevant papers are:

"The Wave Resistance of a Spheroid"[18]

"The Wave Resistance of an Ellipsoid"[19]

"The Moment on a Submerged Body Moving Horizontally"[20]

"The Forces on a Submerged Body Moving Under Waves"[21]

For the present paper, we are interested in wave resistance only, the equations for which are given in Appendices I and II. Since the step from Havelock's equations to numerical results is not entirely trivial, we first checked our results with the only known previous solution, the "slender body" numerical evaluation by Wigley.[22] As Figure 14 shows, the agreement is good.

As recounted in Appendix I, we then compared the theory with tank test measurements of residual resistance; again with satisfactory agreement for our present purposes.

Some general trends were then studied. Figure 15 gives numerical results for a body of revolution, and Figure 16 shows the effect of varying the cross-sectional shape for a fixed submergence of the centerline. The corresponding total resistance ratio is given in Figure 17, and the inverse, L/D in Figure 18. Changing the cross-sectional shape clearly has a very small effect compared with a change in depth, so this effect was ignored in subsequent calculations.

The final calculations are summarized in Figures 3 - 8, which have already been discussed at the beginning of this note.

Some limited work on strut resistance was done during the course of this work, and is summarized in Appendix III. This is considered to be incomplete.

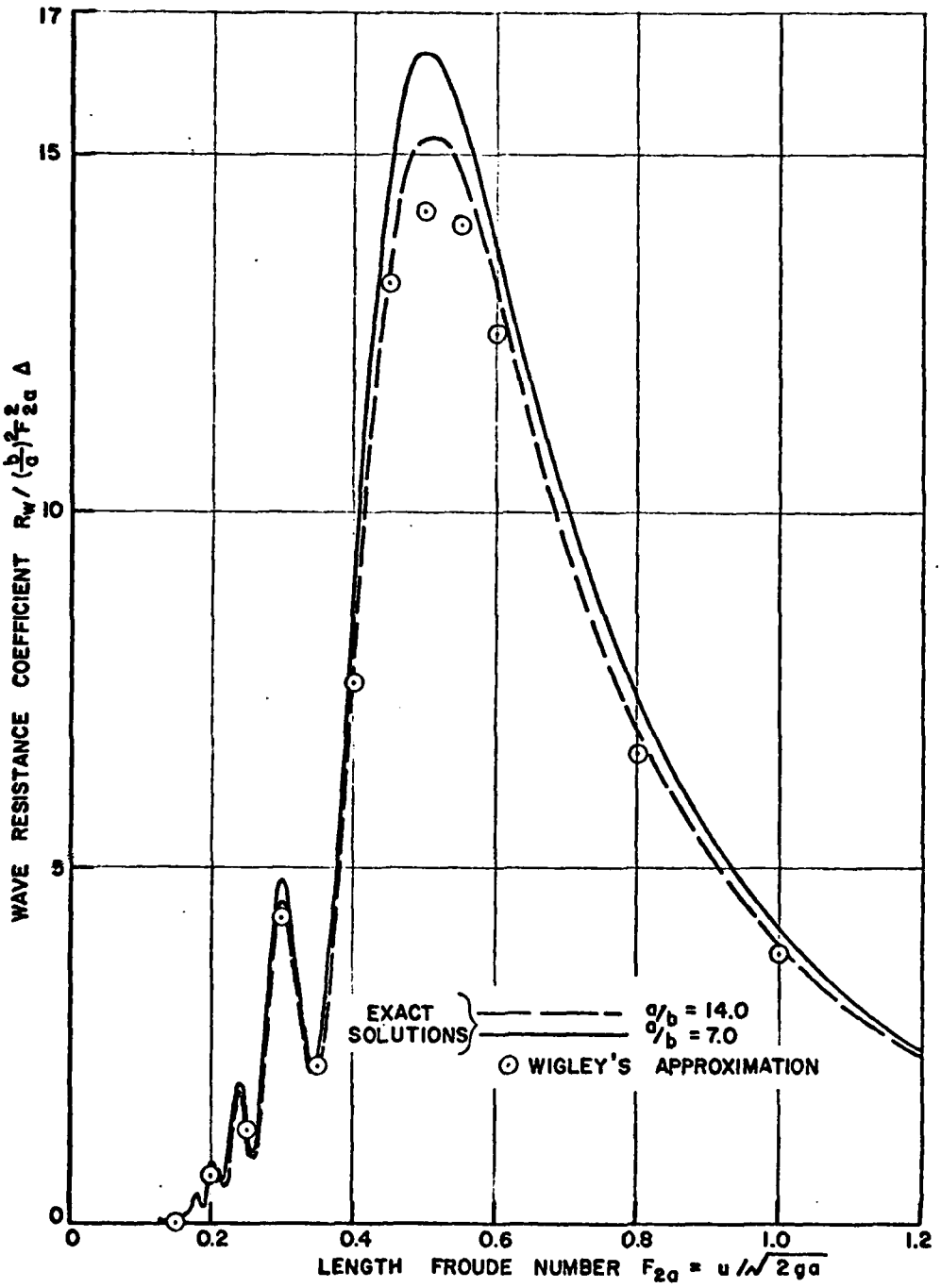

Figure 14. Wigley's "Slender Body" Numerical Approximation in Comparison with the Exact Solution of Havelock's Equation for the Wave Drag of a Prolate Ellipsoid.

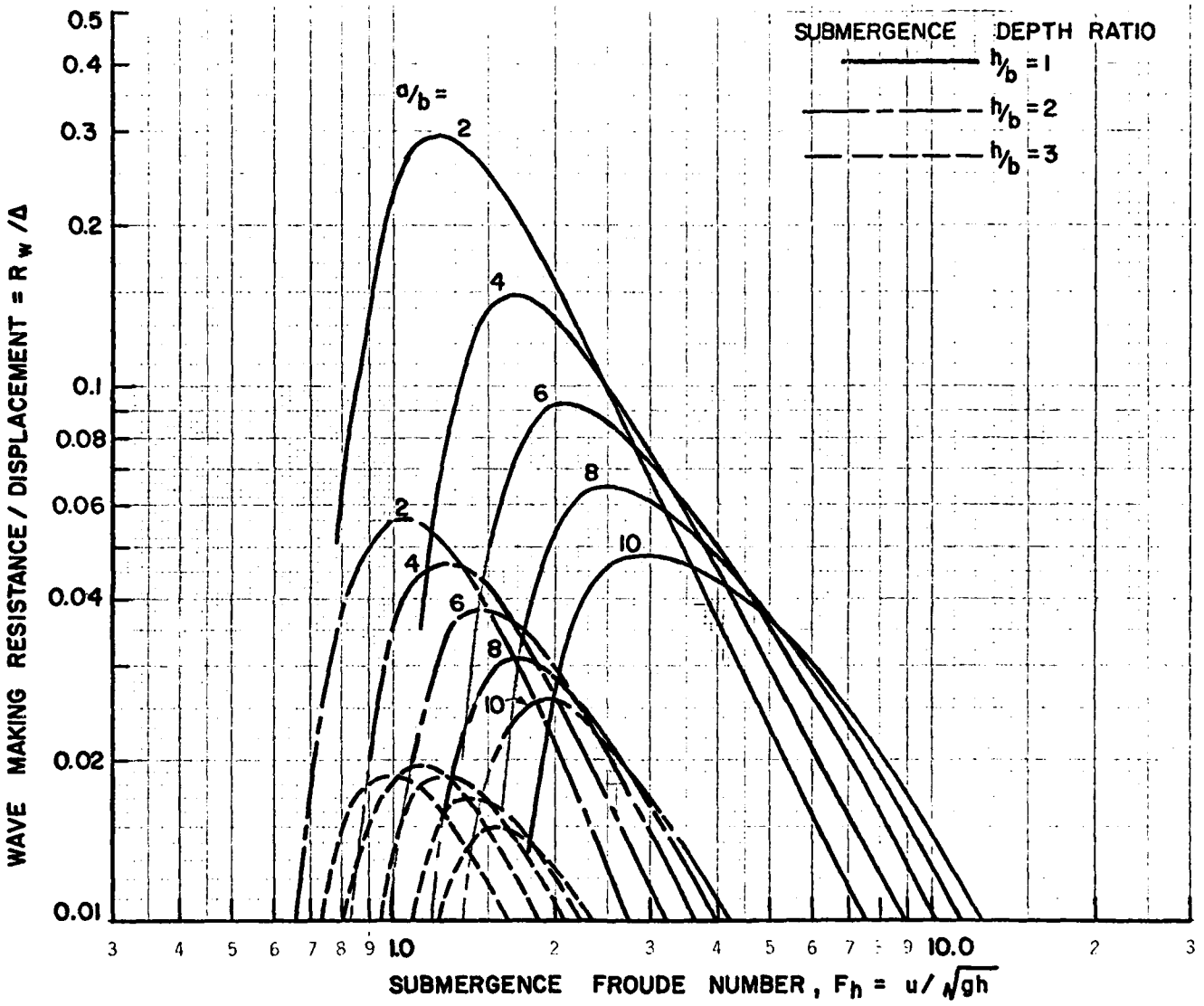

Figure 15. The Effect of Slenderness and Submergence on the Wave Drag of a Prolate Ellipsoid.

$$\frac{h}{b} = \frac{\text{submergence of centerline}}{\text{radius of body}}$$

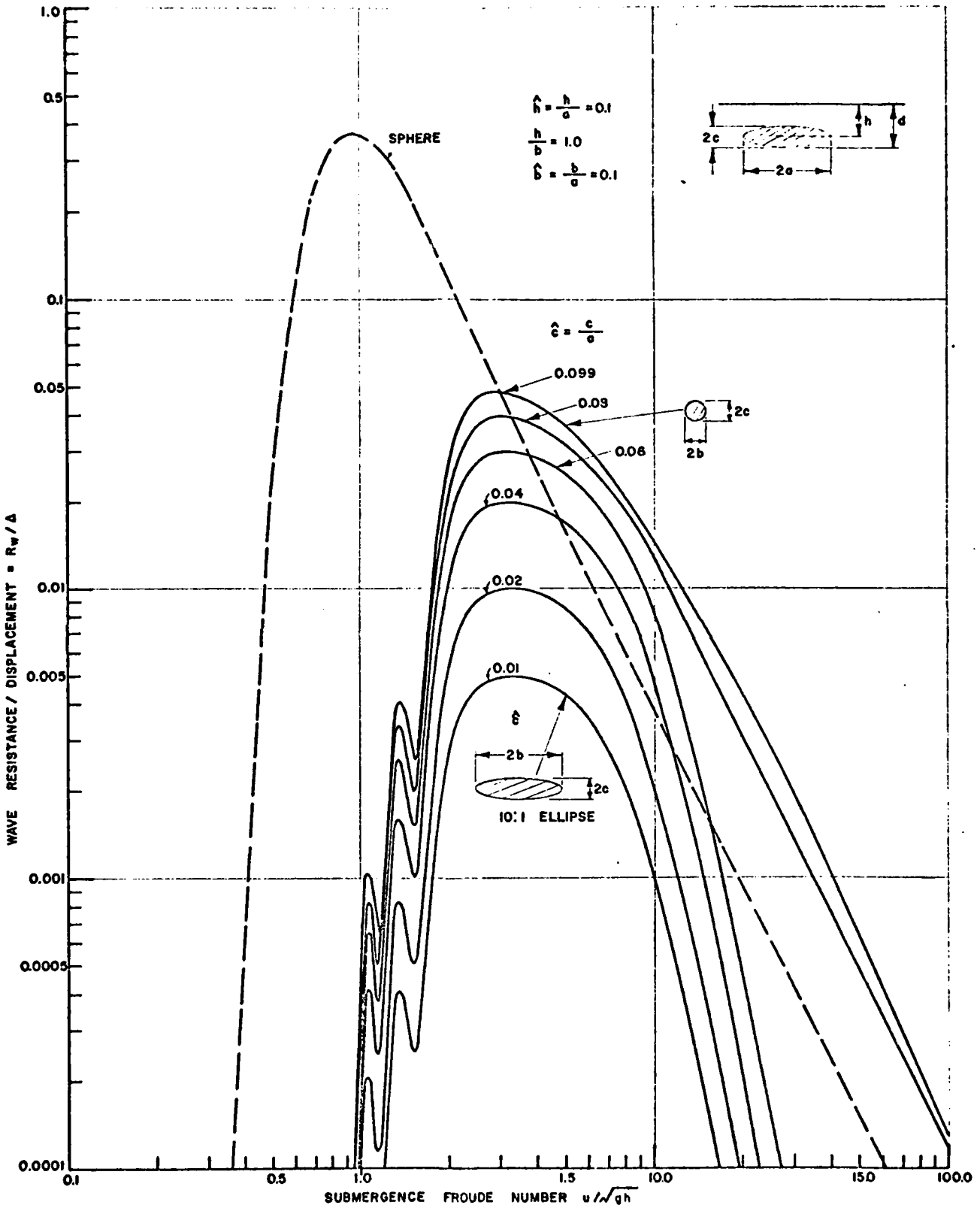

Figure 16. The Effect of Varying the Cross-Section of a Submerged Ellipsoid.

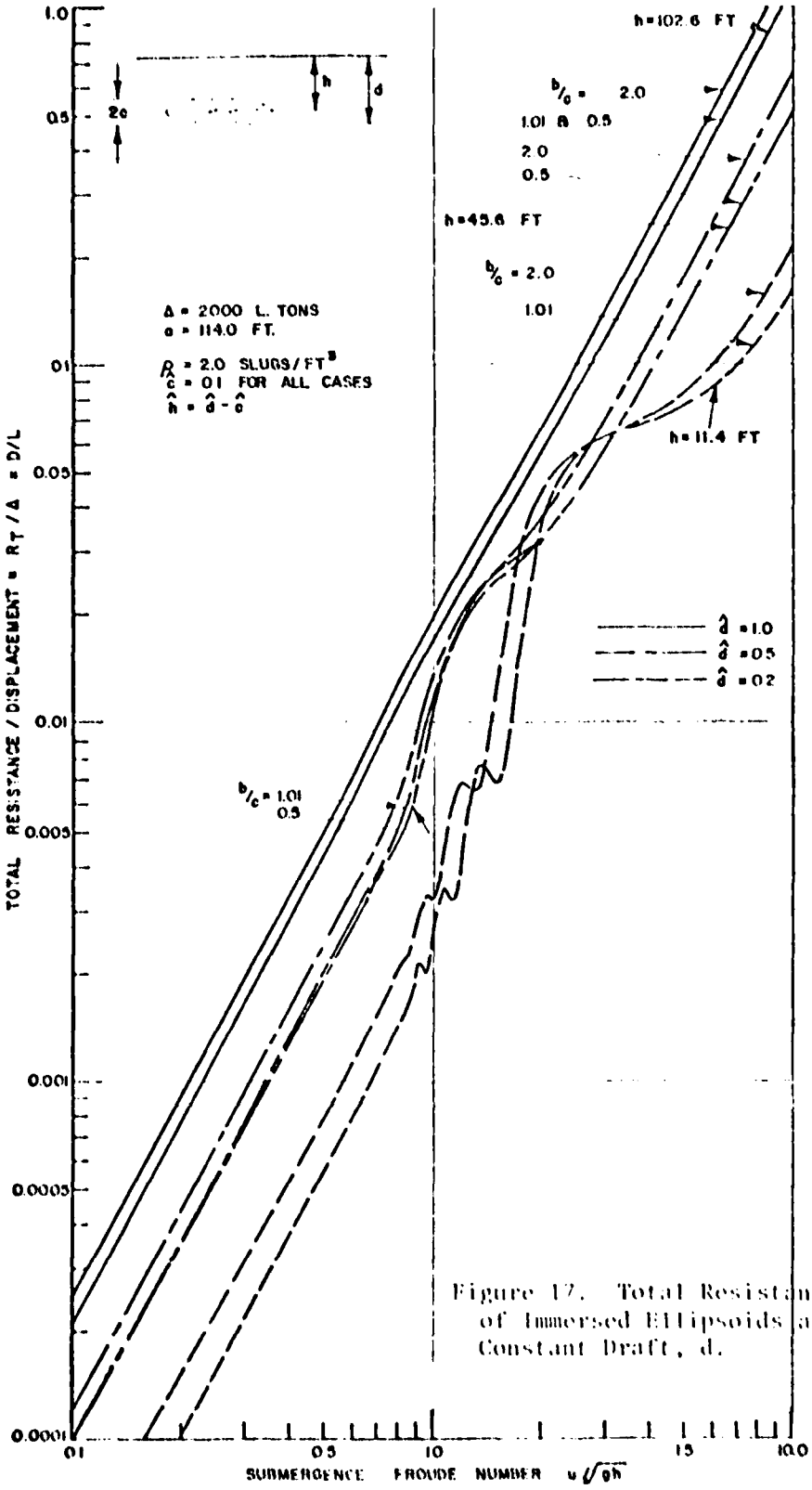

Figure 17. Total Resistance of Immersed Ellipsoids at Constant Draft, d.

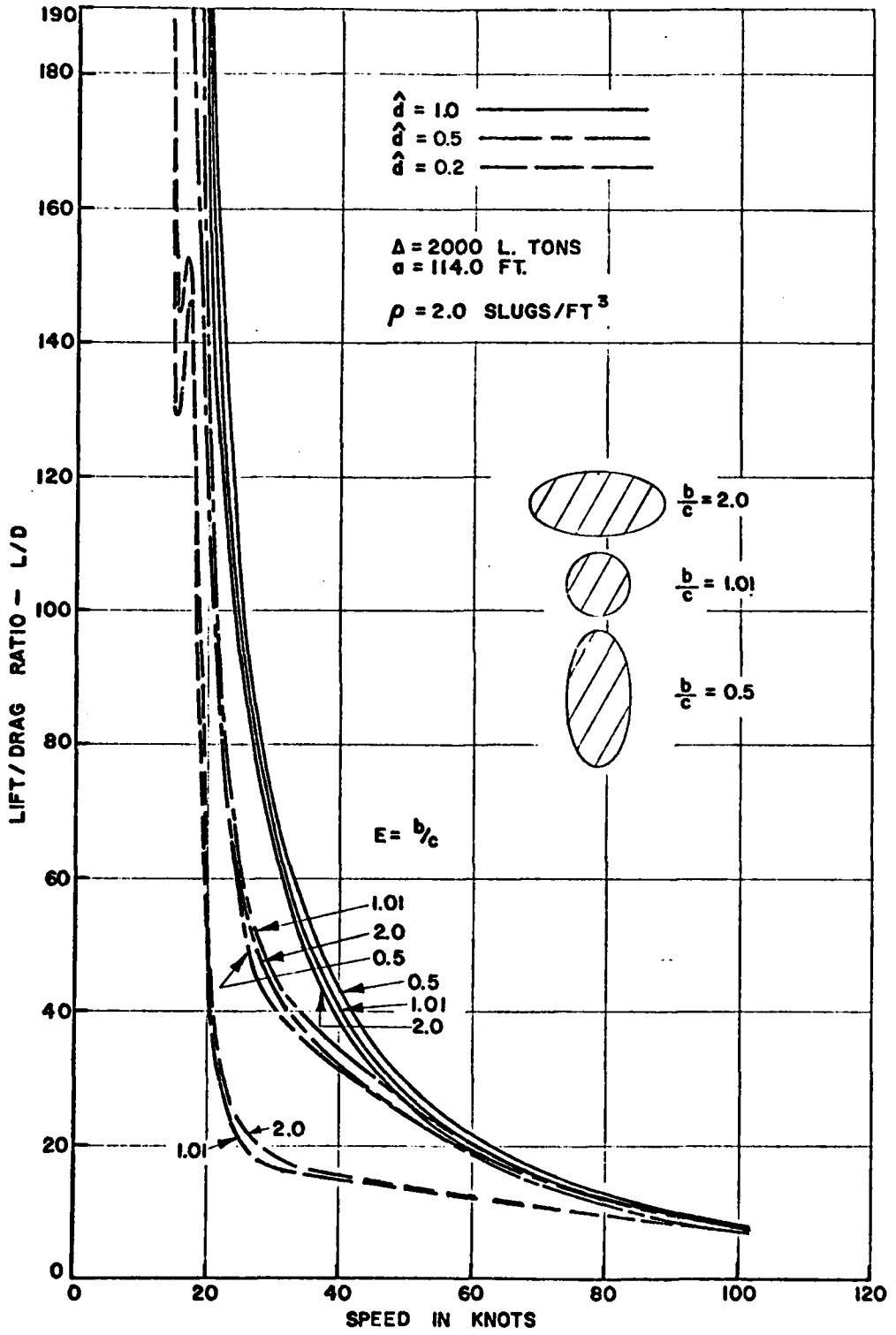

Figure 18. Efficiency of Submerged Ellipsoids at Constant Draft.

REFERENCES

1. Boericke, H., Jr. "Unusual Displacement Hull Forms for Higher Speeds," Int. Shipbuilding Progress, Vol. 6, No. 58 (June 1959).

2. Van Mater, P.R. "A Review of Viscous Friction Prediction Procedures and Viscous Friction Reduction Concepts for Advanced Naval Vehicle Missions in the 1980-2000 Time Period." Payne Inc. Working Paper No. 181-6 (March 1976).

3. Payne, P.R. "Comment on 'Shaping of Axisymmetric Bodies for Minimum Drag in Incompressible Flow'". Journal of Hydronautics, Vol. 9, No. 3 (July 1975).

4. Stratford, B.S. "An Experimental Flow with Zero Skin Friction Throughout its Region of Pressure Rise," Journal of Fluid Mechanics, Vol. 5, Pt. 1 (January 1959).

5. Lewis, E.V. "Ship Speeds in Irregular Waves." Trans. SNAME (1955).

6. Lewis, E.V. "Ship." U.S. Patent 2,974,624 (14 March 1961).

7. Mandel, P. "A Comparative Evaluation of Novel Ship Types." Paper presented at SNAME Spring Meeting (June 1962).

8. Lewis, E.V., and Breslin, J.P. "Semisubmerged Ships for High Speed Operation in Rough Seas," Third Symposium Naval Hydrodynamics, High Performance Ships (ACR-65) (September 1960).

9. Band, E.G.U. "Analysis of Resistance Measurements of FICAT Catamaran Model in Ship Towing Tank and Wind Tunnel." Payne Division of Wyle Laboratories Working Paper No. 1001-6 (November 1968).

10. Payne, P.R. "Application of Michell's Resistance Integral to FICAT Wave Drag." Payne Division of Wyle Laboratories Working Paper No. 1001-3 (October 1968).

11. Payne, P.R. "Squatting of Hulls Which are Half-Bodies of Revolution." Payne Division of Wyle Laboratories Working Paper No. 1001-7 (November 1968).

12. Band, E.G.U. "Evaluation of Michell's Resistance Integral as Adapted to FICAT Wave Drag." Payne Division of Wyle Laboratories Working Paper No. 1001-4 (October 1968).

REFERENCES

13. Leopold, R. "A New Hull Form for High-Speed Volume Limited Displacement-Type Ships." Presented at the SNAME Spring Meeting (May 1969).

14. Leopold, R. "Marine Vessel." U.S. Patent 3,447,502 (June 1969).

15. Marbury, F., Jr. "Small Prototypes of Ships - Theory and Practical Example." Naval Engineers Journal (October 1973).

16. Lang, T.G. "High-Speed Ship with Submerged Hulls." U.S. Patent 3,623,444 (November 1971).

17. Lang, T.G. "Hydrodynamic Design of an S^3 Semi-Submerged Ship." 9th Symposium Naval Hydrodynamics, Vol. 1, Unconventional Ships Ocean Engineering (ACR-203) (August 1972).

18. Havelock, T.H. "The Wave Resistance of a Spheroid." Proc. of the Royal Society A, Vol. 131 (1931).

19. Havelock, T.H. "The Wave Resistance of an Ellipsoid." Proc. of the Royal Society A, Vol. 132 (1931).

20. Havelock, T.H. "The Moment on a Submerged Solid of Revolution Moving Horizontally." Quart. Journal Mech. and Applied Math., Vol. V, Pt. 2 (1952).

21. Havelock, T.H. "The Forces on a Submerged Body Moving Under Waves." Quart Trans. of the Inst. of Naval Architects (1954).

22. Wigley, W.C.S. "Water Forces on Submerged Bodies in Motion." Transactions of the Royal Inst. of Naval Architects, Vol. 95 (1953).

APPENDIX I

CALCULATION OF SMALL WATER PLANE HULL PERFORMANCE

In considering the feasibility of a new ship concept, an early question is "what is its transport efficiency?" We typically evaluate the calm water "lift/drag ratio" (the inverse of the more conventional R/D) in order to answer this, and it's clear that approximate figures for "L/D" are quite adequate for establishing feasibility so long as they are realistic. In the case of S^3, it is rather simple to compute resistance, and it's also clear that, due to small motions in a seaway, performance will not degrade much with increasing sea state; except possibly near resonance.

The significant resistance components are

R_W	Hull wave making drag
D_{BS}	Hull friction drag + Hull pressure drag (considered together in this analysis)
D_{SW}	Strut wave making and spray drag
D_{SS}	Strut skin friction drag + Strut pressure drag
D_i	Strut/hull interference drag
D_A	Wind resistance

The purpose of this Appendix is to present equations for the first three resistance components.

Hull Wavemaking Drag

This is perhaps the most critical term, because it will dominate the optimization of strut length.* On the other hand, it would be needlessly complicated to determine the wave drag of different hull shapes at this stage in the analysis, when we are looking for overall trends. It's sufficient to determine a "standard" variation of wave drag with slenderness ratio and immersion depth, recognizing that subsequent variations of hull volume distribution may enable us to improve on this result.

Such a "standard" variation is provided by Havelock's analysis of a prolate spheroid[I.1], where he obtains

$$R_W = 128\pi^2 g\rho a^3 \epsilon^3 A^2 e^{-2/f^2} \int_0^\infty e^{-2t^2/f^2} \left[J_{3/2}(z)\right]^2 dt \qquad (I.1)$$

* A trade-off which does not seem to have been addressed in the literature.

where

$\epsilon = \sqrt{1 - (b/a)^2}$ the eccentricity

a,b are the major and minor semi-axis lengths

$f = u/\sqrt{gh}$, the submergence Froude number

h = submergence of the spheroid centerline

$J_{3/2}(z)$ is the Bessel Function of the first kind, of order 3/2

$$= \sqrt{2/\pi z}\left(\frac{\sin z}{z} - \cos z\right)$$

$$A = \left[\frac{4\epsilon}{1 - \epsilon^2} - 2 \log \frac{1 + \epsilon}{1 - \epsilon}\right]^{-1}$$

$$z = \frac{\epsilon}{f^2}\left(\frac{a}{h}\right)\sqrt{1 + t^2}$$

t is a dummy variable.

The displacement of a prolate ellipsoid is

$$\Delta = \rho g \frac{4}{3} \pi a b^2 \qquad (I.2)$$

Thus, from equations I.1 and I.2

$$\frac{R_W}{\Delta} = \left\{96\pi\left(\frac{a}{b}\right)^2 \epsilon^3 A^2\right\} e^{-2/f^2} \frac{2}{\pi}\int_0^\infty \frac{e^{-2t^2/f^2}}{z}\left[\frac{\sin z}{z} - \cos z\right]^2 dt \qquad (I.3)$$

The term in the $\{\ \}$ bracket is a function only of b/a and is plotted in Figure I.1, and tabulated in Table I.1.

Equation I.3 is easy to integrate numerically as it stands, so that there is little point in seeking further simplification.* In Figure I.2, we have compared it with some experimental measurements of net residual resistance from Appendix 7 of Reference I.2. Since the experimental data is for "streamline" bodies, the aft portions of which are quite unlike an ellipsoid, the agreement seems excellent, and quite sufficient for our present purposes.

---

* Because of the exponential term, it converges well as t increases.

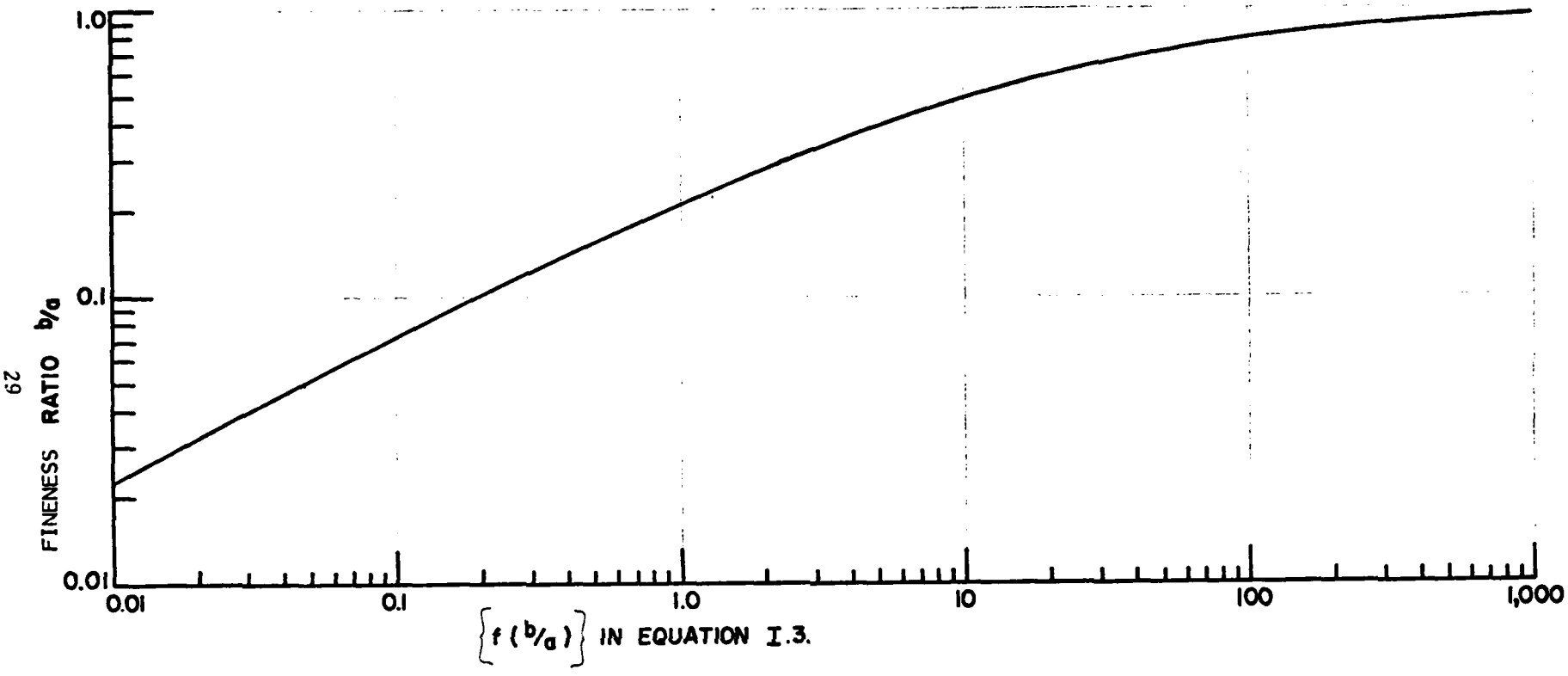

Figure I.1. The Fineness Ratio Term {f(b/a)} in Equation I.3.

Table I.1. Functions of the Fineness Ratio b/a

(b/a)	ε	A	{f(b/a)}
1E-03	.9999995	2.5000211E-07	1.8849846E-05
1E-02	.99995	2.5014505E-05	1.8868605E-03
5E-02	.99874922	6.3161389E-04	4.7946157E-02
1E-01	.99498744	2.5905254E-03	.19936531
.2	.9797959	1.1260011E-02	.89917777
.3	.9539392	2.8651639E-02	2.3880292
.4	.91651514	6.0075642E-02	5.2374138
.5	.8660254	.11643375	10.622599
.6	.8	.22249714	21.234275
.7	.71414284	.44496157	44.383883
.8	.6	1.0231108	106.54675
.9	.43588989	3.5216047	382.42625
.95	.3122499	10.894751	1207.5788
.98	.19899749	45.337269	5086.5397
.99	.14106736	130.40137	14689.081

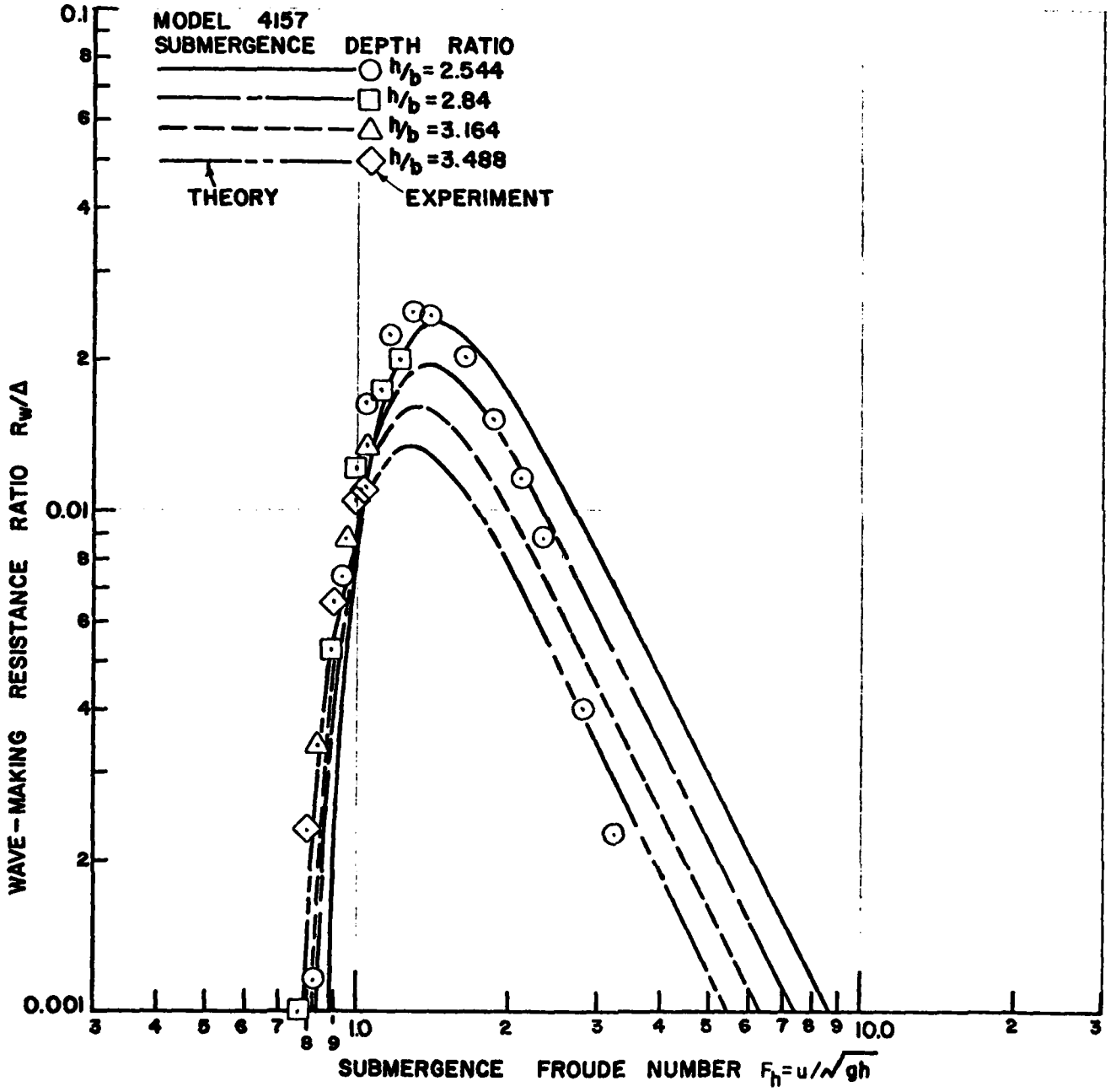

Figure I.2. Comparison Between the Theoretical Wave Drag of a 7:1 Prolate Ellipsoid and Some Experimental Measurements.

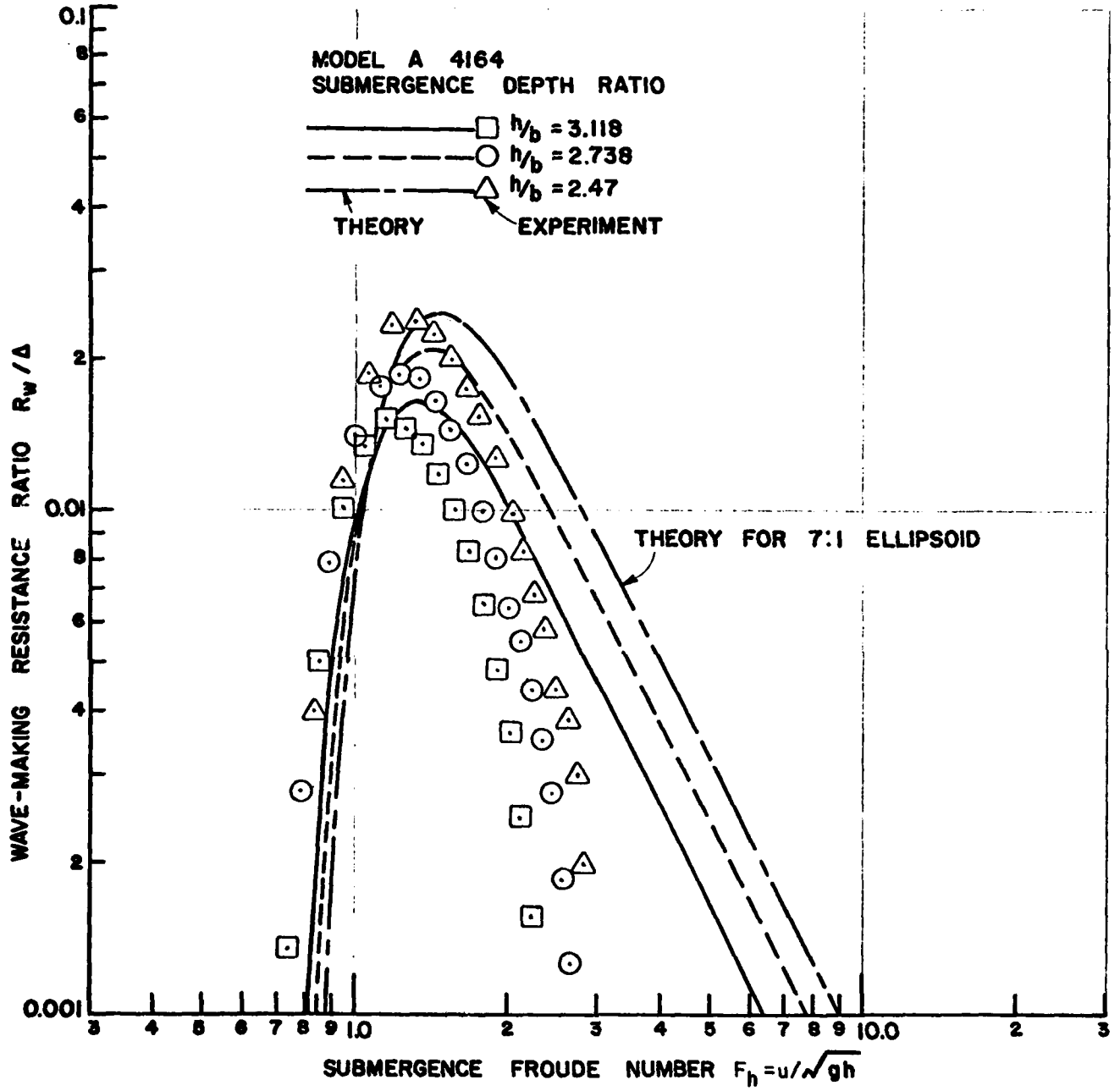

Figure I.2. Continued.

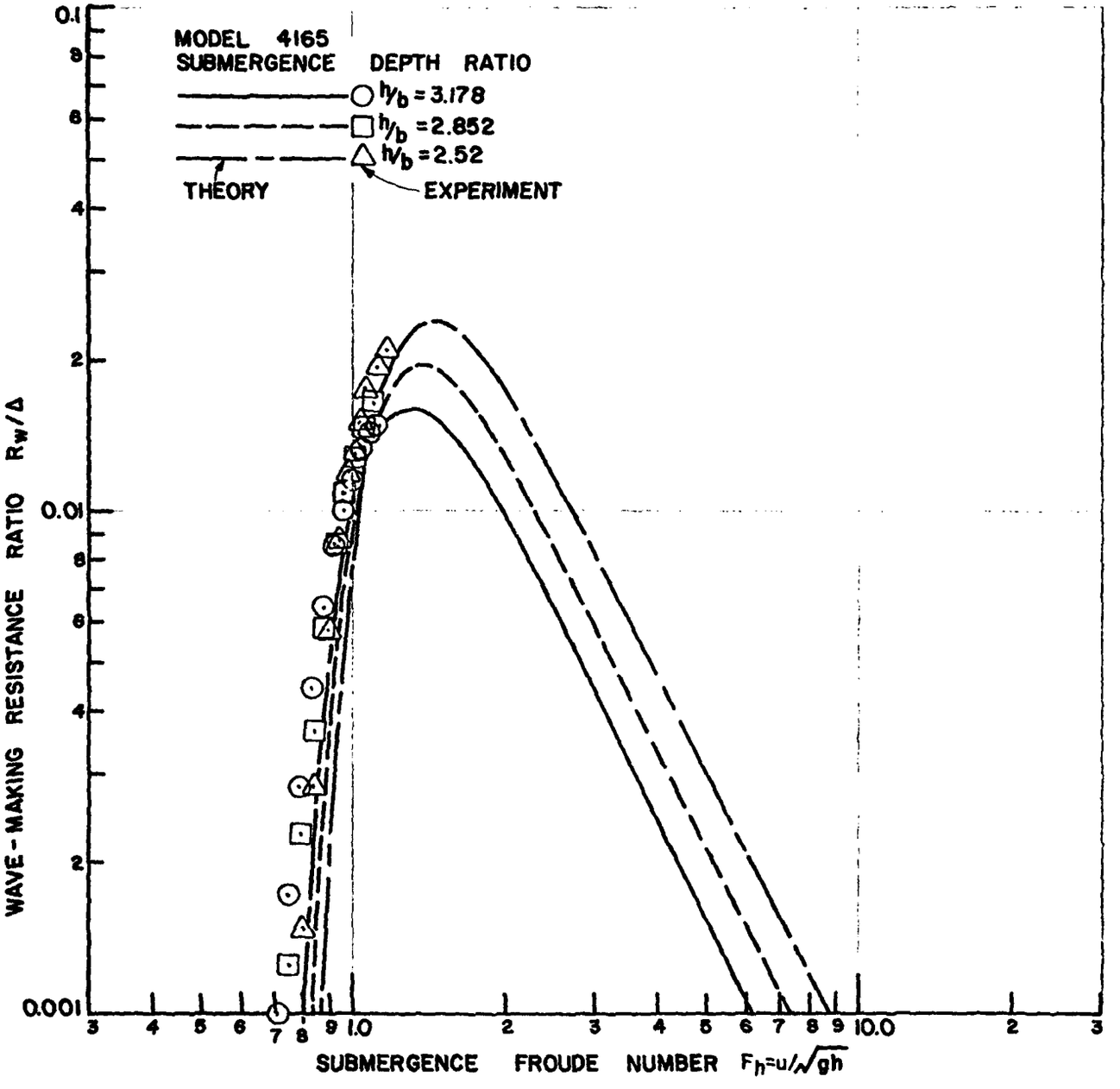

Figure I.2. Continued.

Hull Friction and Pressure Drag

Hoerner[I.3] gives a relationship for this which has been widely accepted. Defining

$$D_{BS} = C_{D_{wet}} \frac{1}{2} \rho u^2 S_{wet} \tag{I.4}$$

$$C_{D_{wet}} = C_{f_B}\left[1 + \frac{3}{2}\left(\frac{b}{a}\right)^{3/2} + 7\left(\frac{b}{a}\right)^3\right] \tag{I.5}$$

where C_{f_B} is the usual flat plate skin friction coefficient, which may be conveniently expressed as

$$C_{f_B} = \frac{0.427}{(\log_{10} R_{2a} - 0.407)^{2.64}} \tag{I.6}$$

$$R_{2a} = \frac{2au}{\nu} \qquad \text{(Reynolds number based on length)} \tag{I.7}$$

$$\nu \simeq 1.25 \times 10^{-5} \ (ft^2/sec) \text{ for normal water}$$

There is no simple relationship between the wetted area S_{wet} and b/a, because other factors are involved, principally the prismatic coefficient,

$$C_P = \frac{\text{Volume}}{2\pi ab^2} \tag{I.8}$$

A typical variation of

$$C_S = \frac{S_{wet}}{4\pi ab} \tag{I.9}$$

with b/a and C_p as given in Figure I.3. C_S is obviously less at the lower prismatics; but then, so is the displacement, so this tends to cancel out. For the purpose of preliminary performance calculations, therefore, we might as well use the spheroid relationship

$$S_{wet} = 2\pi a^2 \left(\frac{b}{a}\right)\left(\frac{b}{a} + \frac{\sin^{-1}\varepsilon}{\varepsilon}\right) \tag{I.10}$$

where

$$\varepsilon = \sqrt{1 - (b/a)^2}$$

Since we are generally working to a given displacement, the hull volume V is known, and since

$$V = \frac{4}{3}\pi a^3 \left(\frac{b}{a}\right)^2 \qquad a = \left(\frac{a}{b}\right)^{2/3}\left(\frac{3V}{4\pi}\right)^{1/3} \tag{I.11}$$

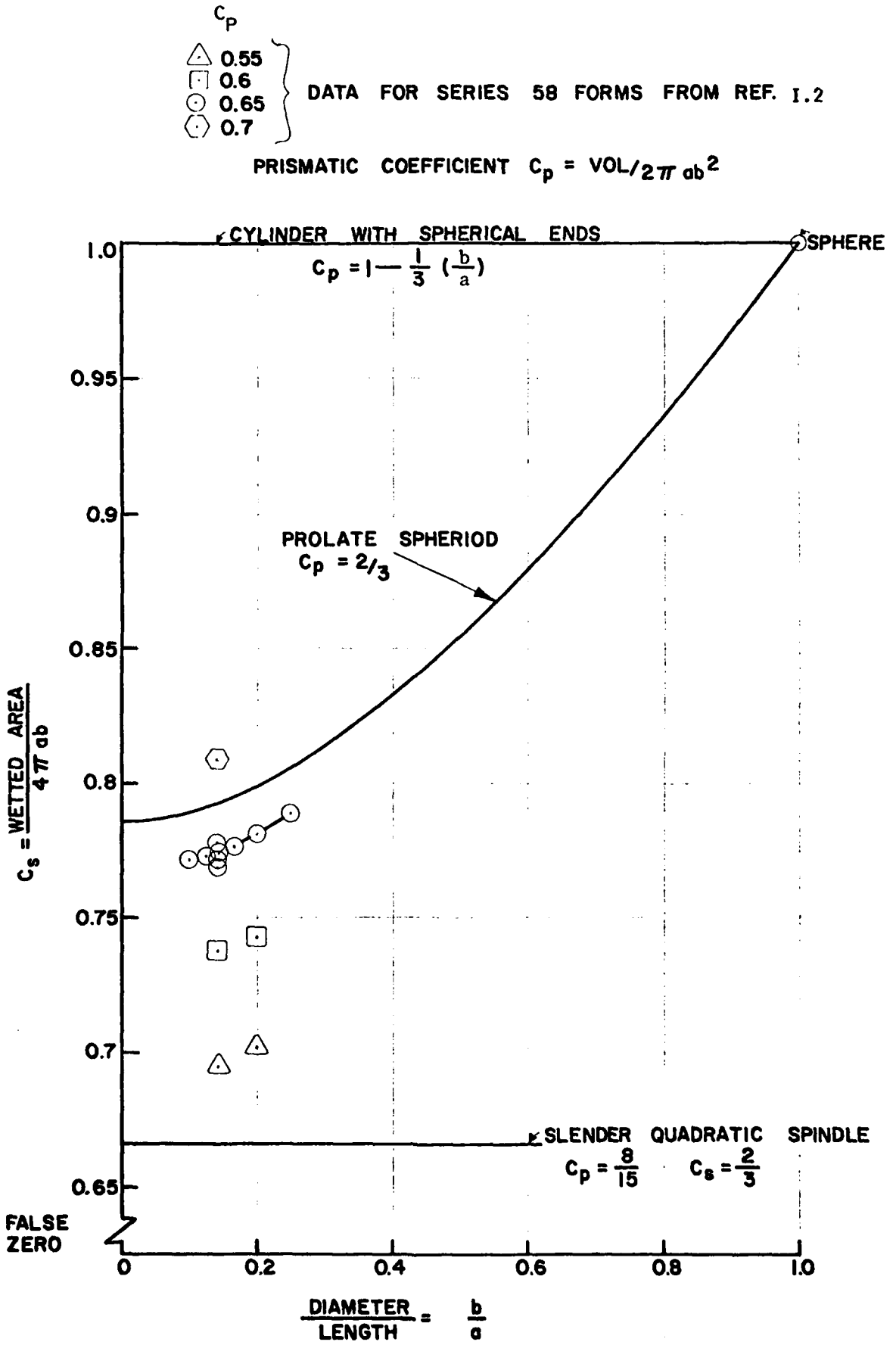

Figure I.3. Wetted Area Coefficient, as a Function of Fineness Ratio and Prismatic Coefficient.

APPENDIX I REFERENCES

I.1 Havelock, T.H. "The Wave Resistance of a Spheroid," Proc. of the Royal Society A, Vol. 131 (1931).

I.2 Gertler, M. "Resistance Experiments on a Systematic Series of Streamlined Bodies of Revolution - for Application to the Design of High Speed Submarines." David W. Taylor Model Basin Report C-297, ATI 86476 (April 1950.

I.3 Hoerner, S.F. Fluid-Dynamic Drag. Published by the Author. (148 Busteed Drive, Midland Park, N.J. 07432). (1965).

APPENDIX II

WAVE RESISTANCE OF SUBMERGED ELLIPSOIDS

The problem of the wave resistance of generalized ellipsoids has been solved by Havelock[II.1]. The purpose of this Appendix is to recast his equations into a form suitable for numerical evaluation.

Case of a > b > c

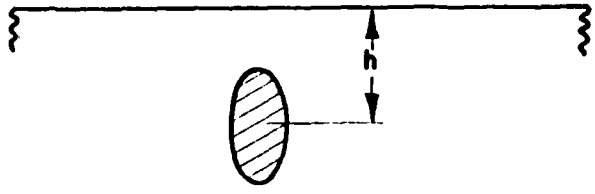

From Havelock[II.1]

$$R_W = \frac{32\pi^2 g\rho a^2 b^2 c^2}{(2-\alpha_o)^2 (a^2-b^2)^{3/2}} e^{-2K_o h}[\text{Int (1)} + \text{Int (2)}] \qquad \text{(II.1)}$$

The volume of the ellipsoid is $\frac{4}{3}\pi abc$. Thus

$$\frac{R_W}{\Delta} = \frac{24\pi abc}{(2-\alpha_o)^2 (a^2-b^2)^{3/2}} e^{-2K_o h}[\text{Int (1)} + \text{Int (2)}] \qquad \text{(II.2)}$$

In Havelock's notation $K_o = g/u^2$. We will employ the submergence Froude number $f = u/\sqrt{gh}$, so that

$$K_o = \frac{g}{f^2 gh} \qquad 2K_o h = 2/f^2 \qquad \text{(II.3)}$$

For numerical integration

$$\alpha_o = abc\int_0^{\lambda_1} \frac{d\lambda}{\sqrt{(a^2+\lambda)^3 (b^2+\lambda)(c^2+\lambda)}} + \frac{2}{3} abc\lambda_1^{-3/2} \qquad \text{(II.4)}$$

where $\lambda_1 >> a^2, b^2, c^2$. (This form of the well known integral is due to Band[II.2].) In nondimensional form, if $\hat{b} = b/a$ $\hat{c} = c/a$ $\hat{\lambda} = \lambda/a^2$

$$\alpha_o = \hat{b}\hat{c}\int_0^{\hat{\lambda}_1} \frac{d\hat{\lambda}}{\sqrt{(1+\hat{\lambda})^3 (\hat{b}^2+\hat{\lambda})(\hat{c}^2+\hat{\lambda})}} + \frac{2}{3}\hat{b}\hat{c}\hat{\lambda}_1^{-3/2} \qquad \text{(II.5)}$$

$$\frac{R_W}{\Delta} = \frac{24\pi\hat{b}\hat{c}}{(2-\alpha_o)^2 (1-\hat{b}^2)^{3/2}} e^{-2/f^2}[\text{Int(1)} + \text{Int(2)}] \qquad \text{(II.6)}$$

Defining

$$\alpha_1^2 = \frac{b^2-c^2}{a^2-b^2} = \frac{\hat{b}^2-\hat{c}^2}{1-\hat{b}^2} \qquad \text{(II.7)}$$

Havelock gives

$$\text{Int}(1) = \int_0^{1/\alpha_1} \frac{\left[J_{3/2}\left\{\frac{1}{f^4h^2}(a^2-b^2)(1+t^2)(1-\alpha_1^2t^2)\right\}^{1/2}\right]^2 e^{-2t^2/f^2}}{(1-\alpha_1^2t^2)^{3/2}}\, dt$$

where the Bessel Function $J_{3/2}$ is defined in Appendix I. Thus the integral can be written as

$$\text{Int}(1) = \frac{2}{\pi}\int_0^{1/\alpha_1} \frac{e^{-2t^2/f^2}}{q} \frac{[(\sin q)/q - \cos q]^2}{(1-\alpha_1^2t^2)^{3/2}}\, dt \qquad \text{(II.8)}$$

where

$$q = \sqrt{\frac{(1-\hat{b}^2)(1+t^2)(1-\alpha_1^2t^2)}{f^4\hat{h}^2}} \qquad \text{(II.9)}$$

$$(\hat{h} = h/a)$$

For the second integral, Havelock gives

$$\text{Int}(2) = \int_{1/\alpha_1}^{\infty} \frac{[I_{3/2}(p)]^2 e^{-2t^2/f^2}}{(\alpha_1^2t^2-1)^{3/2}}\, dt \qquad \text{(II.10)}$$

where

$$p = \sqrt{\frac{(1-\hat{b}^2)(1+t^2)(\alpha_1^2t^2-1)}{f^4\hat{h}^2}} \qquad \text{(II.11)}$$

and $I_{3/2}$ is the modified Bessel Function of the first kind, of order 3/2.

Since

$$I_{1/2}(z) = \sqrt{2/\pi z}\sinh z, \qquad I_{-1/2}(z) = \sqrt{2/\pi z}\cosh z$$

and

$$I_{n+1} = I_{n-1} - \frac{2n}{z} I_n \qquad \text{(a standard form)}$$

$$\therefore\ I_{3/2} = I_{-1/2} - \frac{1}{z} I_{1/2}$$

$$\therefore \quad I_{3/2}(p) = \sqrt{2/\pi p}\ [\cosh(p) - \frac{\sinh(p)}{p}\ ] \tag{II.12}$$

$$\therefore \quad \text{Int}(2) = \frac{2}{\pi}\int_{1/\alpha_1}^{\infty} \frac{e^{-2t^2/f^2}}{p}\ \frac{[\cosh(p) - \frac{\sinh(p)}{p}\ ]^2}{(\alpha_1^2 t^2 - 1)^{3/2}}\ dt \tag{II.13}$$

Equation II.6 can now be evaluated, using equations II.5, II.8 and II.13.

Case of a > c > b

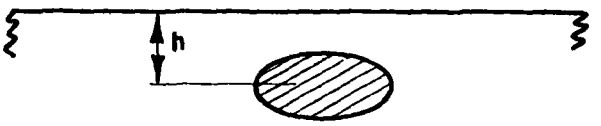

From Havelock, after some manipulation

$$\frac{R_W}{\Delta} = \frac{24\pi\hat{b}\hat{c}\ e^{-2/f^2}}{(2-\alpha_o)^2(1-\hat{b}^2)^{3/2}}\ \text{Int}(3) \tag{II.14}$$

where

$$\text{Int}(3) = \int_o^{\infty} \frac{[J_{3/2}(r)]^2\ e^{-2t^2/f^2}}{(1 + \alpha_2^2 t^2)}\ dt$$

$$= \frac{2}{\pi}\int_o^{\infty} \frac{e^{-2t^2/f^2}}{r}\ \frac{\left(\frac{\sin r}{r} - \cos r\right)^2}{(1 + \alpha_2^2 t^2)^{3/2}}\ dt \tag{II.15}$$

where

$$\alpha_2^2 = \frac{\hat{c}^2 - \hat{b}^2}{1 - \hat{b}^2}$$

and

$$r = \sqrt{\frac{(1-\hat{b}^2)(1+t^2)(1+\alpha^2 t^2)}{f^4 \hat{h}^2}} \tag{II.16}$$

Thus II.14 can be evaluated using II.15 and II.16.

Wave Drag of a Sphere

From Havelock, after some manipulation

$$\frac{R}{\Delta} = \frac{3}{f^6} e^{-2/f^2} \int_0^\infty (1+t^2)^{3/2} e^{-2t^2/f^2} \, dt \qquad (II.17)$$

where $f = u/\sqrt{gh}$, the submergence Froude number.

This solution is a useful check case for the general equations when programmed for numerical solution.

APPENDIX II REFERENCES

II.1	Havelock, T.H.	"The Wave Resistance of an Ellipsoid." Proc. of the Royal Society, A., Vol. 132 (1931).
II.2	Band, E.G.U., and Payne, P.R.,	"The Pressure Distribution on the Surface of an Ellipsoid in Inviscid Flow." Payne Inc. Working Paper No. 101-15 (July 1972).

APPENDIX III

WEDGE STRUT RESISTANCE ESTIMATE

During this study, it was felt that a base-ventilated wedge section strut might have some attractions. Accordingly, the following calculation was carried out.

Surface Pressure Drag

The equations for the force per unit length, P/ℓ, on a wedge are given by Korvin-Kroukovsky and Chabrow[III.1]; viz

$$P/\ell = 2\rho k b v^2 \cos\beta\, f(\gamma) \qquad \text{(III.1)}$$

where

$$\beta = \frac{\pi}{2} - \frac{\theta}{2} \qquad \text{and } \theta \text{ is the wedge included angle}$$

$$f(\gamma) = \int_0^{\pi/2} \left[\left(\frac{1+\sin\gamma}{\cos\gamma}\right)^n - \left(\frac{1+\sin\gamma}{\cos\gamma}\right)^{-n}\right] \cos\gamma \sin\gamma\, d\gamma$$

$$\frac{1}{k} = 4\cos\beta \int_0^{\pi/2} (1+\sin\gamma)^n (\cos\gamma)^{1-n} \sin\gamma\, d\gamma$$

$$n = \frac{\pi - 2\beta}{\pi} = \frac{\theta}{\pi}$$

b is the total strut width

Figure III.1 and Table III.1 give the variation of P with θ obtained from numerical integration of these equations.

Some curve fits to these results are of value.

For $0 < \theta < 30°$

$$C_p = \frac{\theta°}{(89.9543 + 0.517358\ \theta°)}$$

For $0 < \theta < 180°$

$$C_p \simeq 1.1107 \times 10^{-2}(\theta°) - 6.1332 \times 10^{-5}(\theta°)^2 + 2.31799 \times 10^{-7}(\theta°)^3 - 6.02678 \times 10^{-10}(\theta°)^4 + 7.85803 \times 10^{-13}(\theta°)^5$$

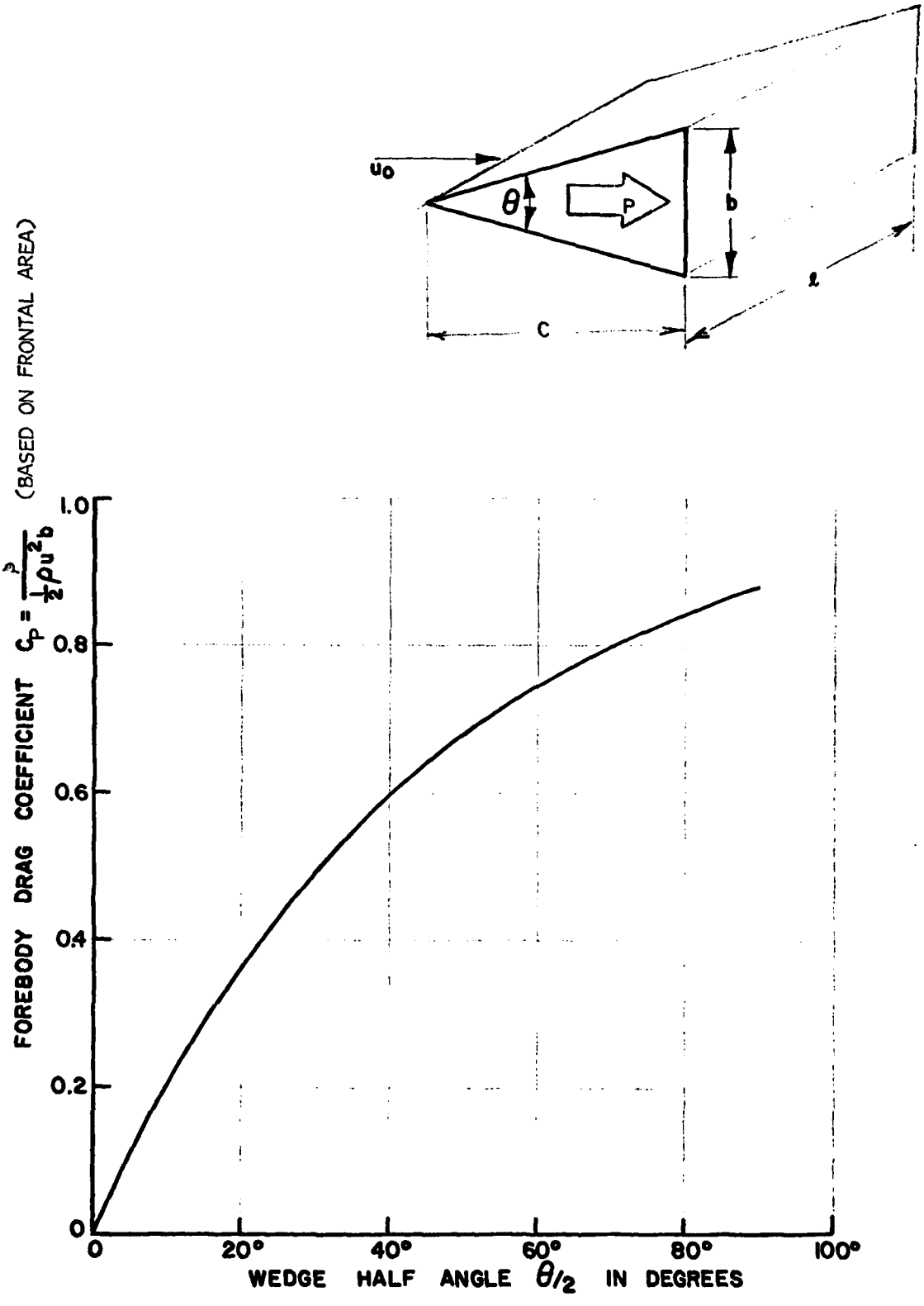

Figure III.1. The Drag Force Acting on the Forward Faces of a Wedge in Two Dimensional Inviscid Flow.

Table III.1

θ (deg.)	C_p
2	0.021978
4	0.043473
6	0.064498
8	0.085062
10	0.105178
12	0.124855
14	0.144104
16	0.162935
18	0.181357
20	0.199379
22	0.217011
24	0.234262
26	0.251140
28	0.267656
30	0.283816
40	0.359552
50	0.427527
60	0.488569
70	0.543405
80	0.592685
90	0.636976
100	0.676800
110	0.712603
120	0.744788
130	0.773720
140	0.799723
150	0.823082
160	0.844058
170	0.862884
180	0.879762

Surface Skin Friction

Korvin-Kroukovsky and Chabrow[III.1] give the surface velocity as

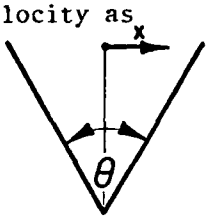

$$\frac{u_s}{u} = \left(\frac{\cos\gamma}{1+\sin\gamma}\right)^n \tag{III.2}$$

where x is related to the dummy variable γ by

$$x = 2kb\cos\beta\int_{\gamma}^{\pi/2}(1+\sin\gamma)^n(\cos\gamma)^{1-n}\sin\gamma\,d\gamma \tag{III.3}$$

In principle, then, we can compute the local skin friction force and integrate it. For the present study, because of time limitations, we employ an approximation which is simpler, although less accurate. We assume that the surface pressure p_s is a constant so that the pressure drag P is given by

$$\frac{P}{b\ell} = p_s - p_\infty \tag{III.4}$$

Since

$$p_\infty + \frac{1}{2}\rho u^2 = p_s + \frac{1}{2}\rho u_s^2$$

$$\frac{1}{2}\rho u_s^2 = p_\infty - p_s + \frac{1}{2}\rho u^2$$

$$= \frac{1}{2}\rho u^2 - \frac{P}{b\ell}$$

$$= \frac{1}{2}\rho u^2\,[1 - C_p] \quad \text{where } C_p = \frac{P}{\frac{1}{2}\rho u^2 b\ell} \tag{III.5}$$

therefore total friction drag

$$D_f \simeq (2c\ell)\,C_f\,\frac{1}{2}\rho u^2\,[1 - C_p] \tag{III.6}$$

where c is the chord and ℓ the wetted length.

Based on frontal area, since

$$c = \frac{b}{2\tan(\theta/2)}$$

$$C_{D_f} = \frac{D_f}{\frac{1}{2}\rho u^2 b\ell} = \frac{C_f}{\tan(\theta/2)}(1 - C_p) \tag{III.7}$$

Base Drag

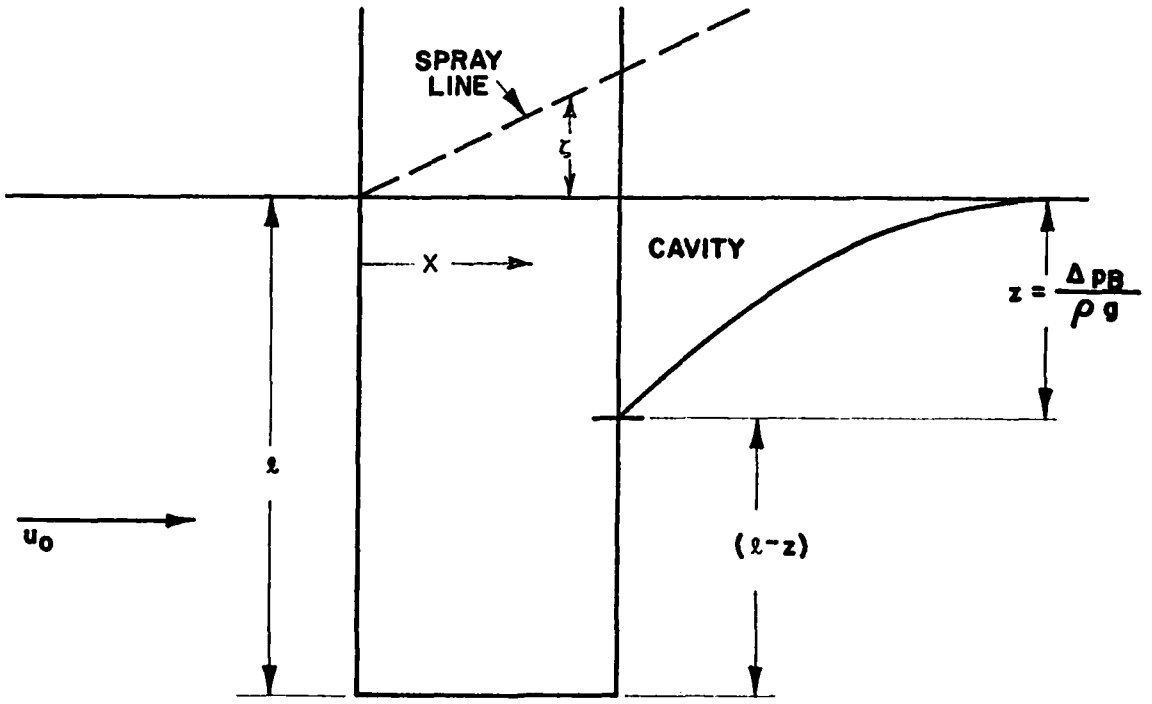

Figure III.2. Side View of Strut.

We can compute the base pressure Δp_B using Hoerner's approximation, or directly from experimental observations. From Hoerner's approximation (p. 3-21)

$$C_{f_B} = \frac{c}{\beta \cos(\theta/2)} C_f = \frac{C_f}{2 \tan(\theta/2) \cos(\theta/2)} \qquad \text{(III.8)}$$

Then

$$\Delta p_B = 0.135 \left(\frac{2 \tan(\theta/2) \cos(\theta/2)}{C_f} \right)^{1/3} \frac{1}{2} \rho u^2 \qquad \text{(III.9)}$$

As Figure III.3 shows, this agrees well with experimental observations.

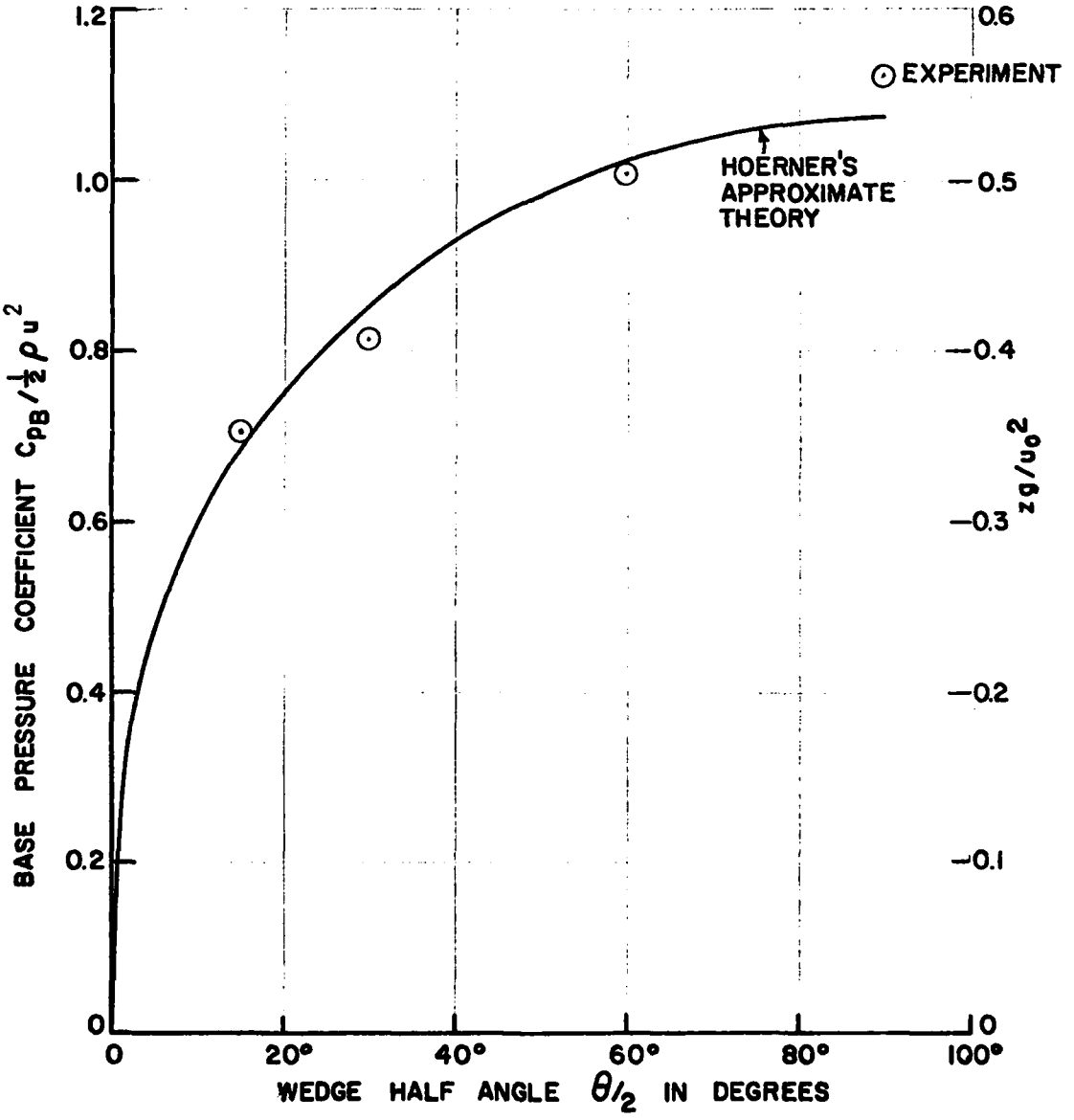

Figure III.3. Comparison Between Hoerner's Approximation for Base Drag Pressure, and $C_{P_B} = C_D - C_P$, where C_P is determined from Figure III.1, and C_D from Hoerner's Summary of Experimental Data. (C_f = .004)

The depth z of the ventilation is then given by

$$\Delta p_B = \rho g z$$

i.e.

$$\frac{zg}{u^2} = 0.0675 \left(\frac{2 \tan (\theta/2) \cos (\theta/2)}{C_f} \right)^{1/3} \qquad \text{(III.10)}$$

This is plotted as an equivalent Froude number in Figure III.4.

$u/\sqrt{gz}$ is a kind of Froude number, therefore, dependent only upon θ and C_f. Typical values are:

For $C_f = .004$, $\theta/2 = 5°$ and

u =	10	20	30	40	50	knots
z =	2.1	8.4	18.9	33.6	52.5	ft

The total base drag of the strut will be

$$D_B = \left(\frac{1}{2} z\rho g\right) bz + b(\ell - z)\, \Delta p_B$$

$$= \frac{1}{2} \rho g b z^2 + b(\ell - z)\, \frac{1}{2} \rho u^2 \, \frac{zg}{2u^2}$$

$$= \frac{1}{2} \rho g b z^2 + \frac{1}{4} \rho g b z (\ell - z)$$

$$= \frac{1}{4} \rho g b (z^2 + \ell z) \qquad \text{(III.11)}$$

where

z is given by equation III.10.

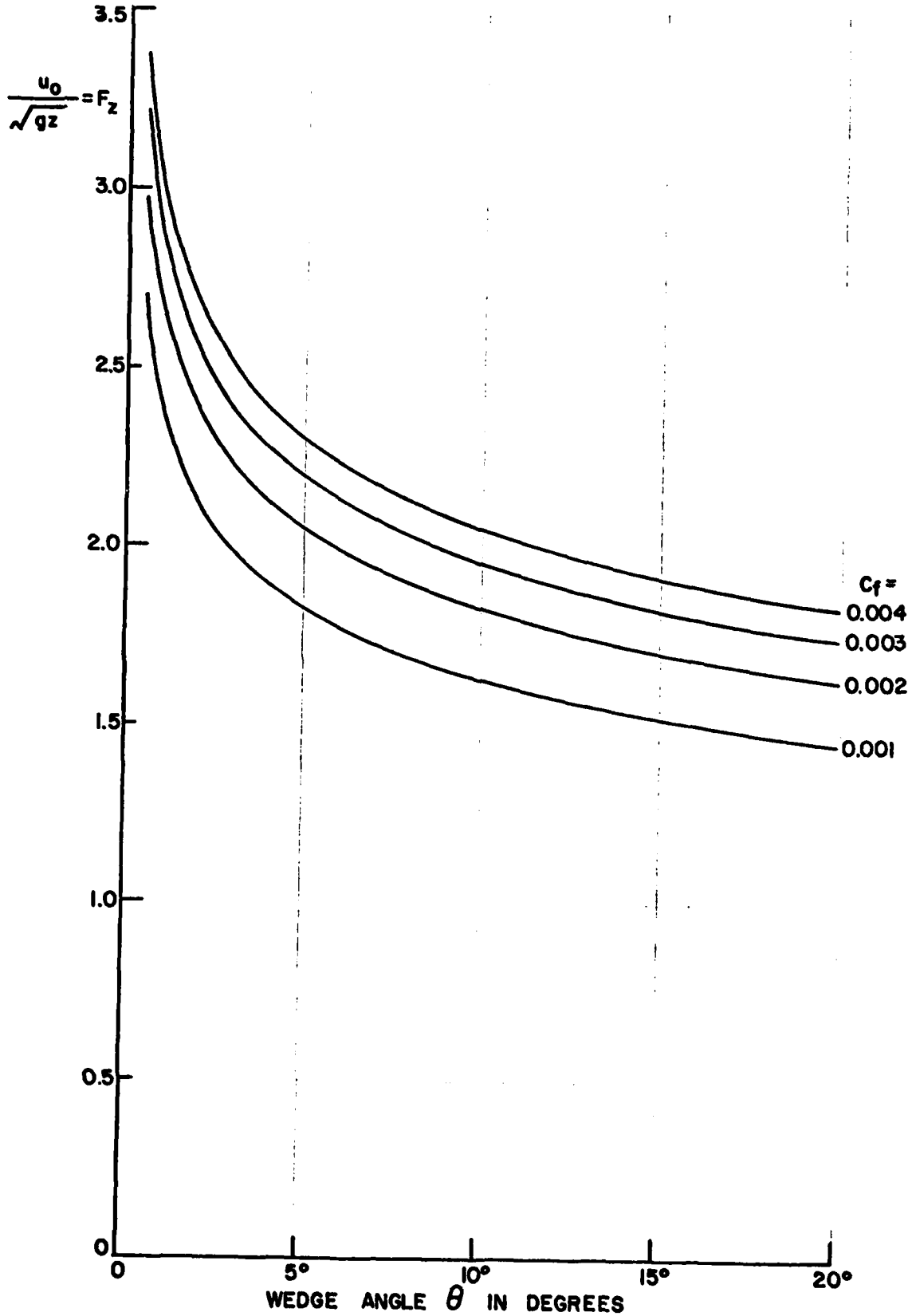

Figure III.4. Ventilation Froude Number as a Function of Wedge Angle.

Spray Drag

From Ogilvie[III.2] we take the spray surface elevation to be (see Figure III.2)

$$\zeta = \frac{\theta}{\pi}\int_0^\infty \cos(\theta x\lambda/2)\left[\frac{1-e^{-H\lambda}}{\lambda}\right]\left[\frac{\sin(\sqrt{K\lambda}\,x)}{\sqrt{K\lambda}}\right]d\lambda \qquad \text{(III.12)}$$

where $K = g/u^2$

The wetted area associated with this is

$$\Delta S = \int_0^x \zeta\, dx \qquad \text{(III.13)}$$

In the numerical integration of equation III.12, a singularity occurs at $\lambda = 0$. This difficulty can be avoided by integrating to infinity from a small value λ_1, and determining the residue as follows. Since $\lambda_1 << 1$, $\cos(\theta x\lambda/2) \simeq 1.0$, except right at the bow ($x = 0$). Also $\sin(\sqrt{K\lambda}\,x) = \sqrt{K\lambda}\,x$.

$$\therefore \Delta\zeta = \frac{\theta}{\pi}\int_0^{\lambda_1}\left(\frac{1-e^{-H\lambda}}{\lambda}\right)x\,d\lambda$$

$$\simeq \frac{\theta x}{\pi}\int_0^{\lambda_1}\left(\frac{H\lambda}{1!}-\frac{(H\lambda)^2}{2!}+\frac{(H\lambda)^3}{3!}-\frac{(H\lambda)^4}{4!}+\cdots\right)\frac{d\lambda}{\lambda}$$

$$\frac{\theta x}{\pi}\left[H\lambda_1-\frac{(H\lambda_1)^2}{2.2!}+\frac{(H\lambda_1)^3}{3.3!}-\frac{(H\lambda_1)^4}{4.4!}+\cdots\right] \qquad \text{(III.14)}$$

Equation III.12 is plotted in Figure III.5 for some arbitrary values of H and x.

Total Strut Resistance

If $z < \ell$ (or $gz/u^2 < g\ell/u^2$, or $u^2/gz > u^2/g\ell$)

$$D = \frac{1}{2}\rho u^2 b\ell C_p + \frac{1}{2}\rho u^2 C_f \frac{b\ell}{\tan(\theta/2)}(1-C_p$$

$$+\left\{\frac{1}{2}\rho g z^2 b + b(\ell-z)\frac{1}{2}\rho u^2 (zg/2u^2)\right\} + (\text{spray drag}) \qquad \text{(III.15)}$$

From Ogilvie[III.2]

$$\zeta(X,0) = \frac{2\theta}{\pi}\sqrt{\ell/K}\; Z(X,0)$$

$$Z(X,0) = \int_0^\infty \frac{1 - e^{-u}}{u}\;\frac{\sin \mathcal{X}\sqrt{u}}{\sqrt{u}}\; du$$

$$\mathcal{X} = X\sqrt{K/H}$$

$$K = g/u^2$$

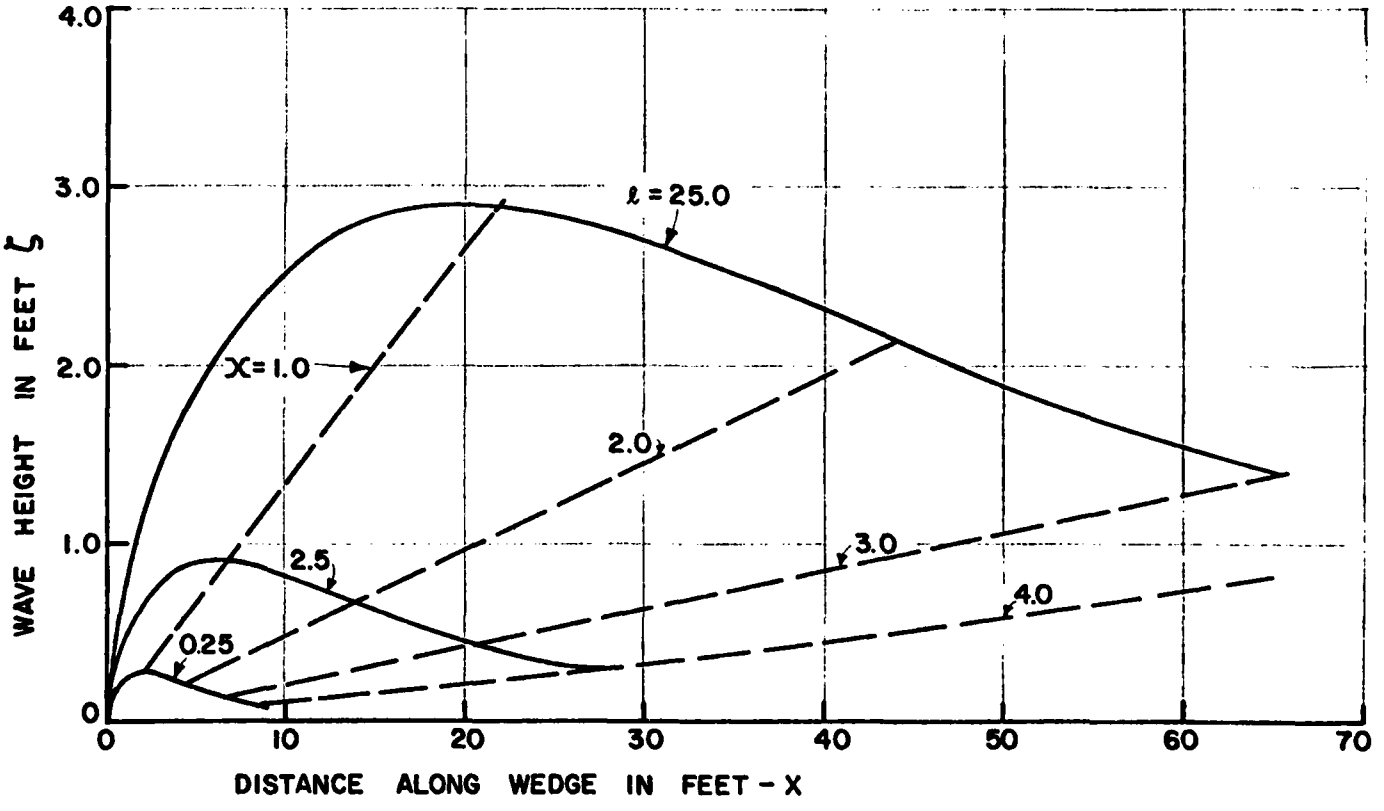

Figure III.5. Spray Sheet Surface Elevation from Equation III.12.
ℓ = Draft in feet
This case is for u = 25 ft/sec, θ = 7.5°

If $u^2/gz < u^2/g\ell$ the terms in the curly bracket become

$$\left\{ \frac{1}{2} \rho g \ell^2 b \right\} \qquad \text{(III.15a)}$$

If we base C_D on $\frac{1}{2} \rho u^2 b\ell$

$$C_D = C_P + \frac{C_f}{\tan (\theta/2)} (1 - C_P) + \frac{1}{2} \left\{ \left(\frac{gz}{u^2} \right)^2 \frac{u^2}{g\ell} + \frac{gz}{u^2} \right\} \qquad \text{(III.16)}$$

or

$$+ \text{(spray drag)}$$

$$\left\{ \frac{g\ell}{u^2} \right\} \qquad (\text{for } u^2/gz < u^2/g\ell)$$

Note that

$$\frac{gz}{u^2} = 0.0675 \left(\frac{2 \tan (\theta/2) \cos (\theta/2)}{C_f} \right)^{1/3} \qquad \text{(III.10)}$$

Some typical results are given in Figure III.6. Spray drag has been omitted from the calculation because of time limitations.

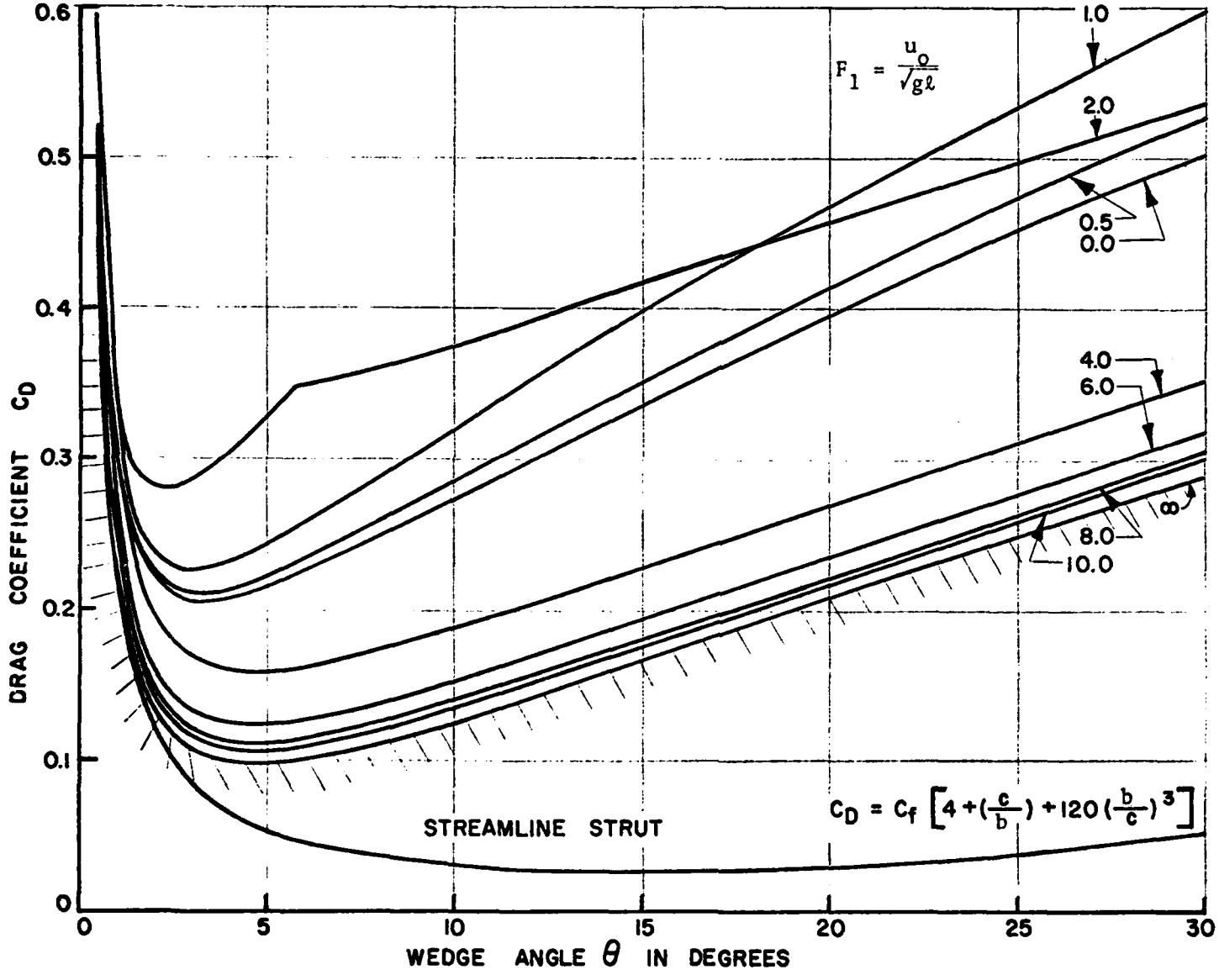

Figure III.6. Total Resistance (Less Spray Drag) of a Vented Strut, Assuming C_f = .002.

APPENDIX III REFERENCES

III.1	Korvin-Kroukovsky, B.V., and Chabrow, F.R.	"The Discontinuous Fluid Flow Past an Immersed Wedge." Sherman M. Fairchild Publication Fund Paper Preprint No. 169 (October 1948).
III.2	Ogilvie, T.F.	"The Wave Generated by a Fine Ship Bow." Proc. Ninth Symposium on Naval Hydrodynamics (1972). Also: Report No. 127, DNAME, Univ. of Michigan (1973).